Received: 2 February 2024 | Revised: 15 August 2024 | Accepted: 21 September 2024

DOI: 10.1002/alz.14347

Alzheimer's & Dementia®
THE JOURNAL OF THE ALZHEIMER'S ASSOCIATION

RESEARCH ARTICLE

Transcriptomic and epigenomic profiling reveals altered responses to diesel emissions in Alzheimer's disease both in vitro and in population-based data

Liudmila Saveleva[1] | Tereza Cervena[2,3] | Claudia Mengoni[4] | Michal Sima[3] | Zdenek Krejcik[2] | Kristyna Vrbova[3] | Jitka Sikorova[2] | Laura Mussalo[1] | Tosca O. E. de Crom[5] | Zuzana Šímová[3] | Mariia Ivanova[1] | Muhammad Ali Shahbaz[1] | Elina Penttilä[6] | Heikki Löppönen[6] | Anne M. Koivisto[7,8,9] | M. Arfan Ikram[5] | Pasi I Jalava[10] | Tarja Malm[1] | Sweelin Chew[1] | Michal Vojtisek-Lom[2,11,12] | Jan Topinka[2] | Rosalba Giugno[4] | Pavel Rössner[3] | Katja M. Kanninen[1]

[1]A. I. Virtanen Institute for Molecular Sciences, University of Eastern Finland, Kuopio, Finland

[2]Department of Genetic Toxicology and Epigenetics, Institute of Experimental Medicine of the Czech Academy of Sciences, Prague, Czech Republic

[3]Department of Nanotoxicology and Molecular Epidemiology, Institute of Experimental Medicine of the Czech Academy of Sciences, Prague, Czech Republic

[4]Department of Computer Science, University of Verona, Verona, Italy

[5]Department of Epidemiology, Erasmus MC, University Medical Center, Rotterdam, The Netherlands

[6]Department of Otorhinolaryngology, University of Eastern Finland and Kuopio University Hospital, Kuopio, Finland

[7]Department Driving Assessment, Neuro Centre, Kuopio University Hospital, Kuopio, Finland

[8]Department of Geriatrics, Helsinki University Hospital, Helsinki, Finland

[9]Department of Neurosciences, Faculty of Medicine, University of Helsinki, Helsinki, Finland

[10]Department of Environmental and Biological Sciences, University of Eastern Finland, Kuopio, Finland

[11]Department of Mechatronics and Computer Engineering, the Technical University of Liberec, Liberec, Czech Republic

[12]Faculty of Mechanical Engineering, Czech Technical University in Prague, Prague, Czech Republic

Correspondence
Katja M. Kanninen, A.I. Virtanen Institute for Molecular Sciences, University of Eastern Finland, Neulaniementie 2, 70210 Kuopio, Finland.
Email: katja.kanninen@uef.fi

Funding information
ADAIR project, Grant/Award Number: JPND2019-466-037; Czech Science Foundation, Grant/Award Number: 22-10279S; Ministry of Education, Youth, and Sports of the Czech Republic; European Union—European Structural and Investments Funds in the frame of Operational Programme Research Development and Education,

Abstract

INTRODUCTION: Studies have correlated living close to major roads with Alzheimer's disease (AD) risk. However, the mechanisms responsible for this link remain unclear.

METHODS: We exposed olfactory mucosa (OM) cells of healthy individuals and AD patients to diesel emissions (DE). Cytotoxicity of exposure was assessed, mRNA, miRNA expression, and DNA methylation analyses were performed. The discovered altered pathways were validated using data from the human population-based Rotterdam Study.

RESULTS: DE exposure resulted in an almost four-fold higher response in AD OM cells, indicating increased susceptibility to DE effects. Methylation analysis detected different DNA methylation patterns, revealing new exposure targets. Findings were

Grant/Award Number: CZ.02.1.01/0.0/0.0/16_013/0001821; Doctoral Program in Molecular Medicine at the University of Eastern Finland; Kuopio University Foundation,; North Savo Regional Fund of the Finnish Cultural Foundation, Grant/Award Number: 65231471; Stichting Erasmus Trustfonds, Grant/Award Number: 97030.2021.101.430/057/RB; Netherlands Organisation for Health Research and Development, Grant/Award Number: 733051107; Pohjois-Savon Rahasto, Grant/Award Number: n/a; EU Joint Programme – Neurodegenerative Disease Research, Grant/Award Number: JPND2019-466-037

validated by analyzing data from the Rotterdam Study cohort and demonstrated a key role of nuclear factor erythroid 2–related factor 2 signaling in responses to air pollutants.

DISCUSSION: This study identifies air pollution exposure biomarkers and pinpoints key pathways activated by exposure. The data suggest that AD individuals may face heightened risks due to impaired cellular defenses.

KEYWORDS

air pollution, air–liquid interface (ALI), Alzheimer's disease (AD), heat shock protein (HSP), next-generation sequencing (NGS), nuclear factor erythroid 2–related factor 2 (NRF2), traffic emissions, traffic-related air pollution (TRAP) olfactory mucosa (OM)

Highlights

- Healthy and AD olfactory cells respond differently to DE exposure.
- AD cells are highly susceptible to DE exposure.
- The NRF2 oxidative stress response is highly activated upon air pollution exposure.
- DE-exposed AD cells activate the unfolded protein response pathway.
- Key findings are also confirmed in a population-based study.

1 | BACKGROUND

According to the World Health Organization, millions of deaths are attributed to air pollution annually.[1] A mounting body of research indicates that air pollution has adverse effects on many organs, including the brain.[2,3] Living in areas with poor air quality is associated with an increased risk of cognitive decline and neurodegenerative diseases, including Alzheimer's disease (AD).[4,5] Air pollution exposure is linked to the occurrence of AD-like pathology and the disease progression in both people and animal models, as summarized in.[6] Recently, air pollution has been added to the list of the 12 modifiable risk factors for dementia, which account for approximately 40% of dementia cases globally.[7] Therefore, further understanding of the impact of air pollution exposure can have a significant impact on disease prevention. However, the fundamental cellular and molecular mechanisms induced by exposure, impacts on the brain, and connection to AD remain poorly understood.

Olfactory mucosa (OM) cells in the upper nasal cavity control olfaction. The OM is among the first tissues to be exposed to inhaled air, and as a result, it is subjected to a wide range of toxins. Importantly, the OM has a direct connection to the brain through the olfactory nerve. Considering that recent evidence shows a decline in human olfaction after exposure to air pollution[8] and olfaction impairment is a typical early symptom of neurodegenerative diseases like AD, it is crucial to concentrate research efforts on deciphering the molecular and cellular events linking environmental contaminants and the OM.

Studies on the neurotoxic effects of pollutants have focused in particular on the nose-to-brain transfer pathway,[9] with most of the olfactory system investigations conducted to date using animal models. Specifically, exposure to diesel exhaust (DE) particles has been shown to reduce sniffing and alter the expression of several genes in mouse nasal tissue.[10] However, in comparison to rodent cells, human cells are known to respond with greater magnitude to certain components of traffic-related air pollutants (TRAP).[11] To investigate the impact of TRAP on the human olfactory system,[12] we used a highly translational research model of human primary OM cells obtained from nasal biopsies, characterized previously.[13] This cell model maintains certain disease-related features of AD[13] and represents several homeostasis deficiencies observed in the AD brain, highlighting its translational potential.[14] Recently, using a submerged culture mode of OM cells, we revealed that exposure to TRAP attenuated gene expression profiles in cells obtained from healthy donors.[15] Here, to better mimic a real-life exposure scenario, we exposed cells to complete DE at an air–liquid interface (ALI). The exposure system, along with its advantages over both in vitro and in vivo exposure techniques, was previously described.[16] We hypothesized that ALI exposure to complete DE would induce alterations in the OM cell transcriptome and methylation level and differentially affect non-demented subjects and individuals with AD. The specific aims of the study were to (i) identify key molecular mechanisms affected by DE exposure in OM cells and (ii) evaluate how existing AD pathology influences the responses of cells exposed to complete DE in ALI. Additionally, we assessed data from the prospective population-based Rotterdam Study aiming to validate differentially expressed genes (DEGs) and pathways found in the in vitro experiment. Data from plasma samples collected from 2657 study participants were classified based on AD diagnosis and additionally divided into participants living in highly polluted areas and lower polluted areas. The main tasks performed in the Rotterdam Study aimed at (i) identifying biomarkers that were differential in AD compared to controls, (ii) identifying biomarkers of differential air pollution data, and

RESEARCH IN CONTEXT

1. **Systematic review**: The study addresses a pressing problem: the interplay of air pollution and AD. Air pollution is a vast global health concern, with increasing evidence linking it to AD. However, the exact molecular mechanisms involved are yet to be described. A better understanding of this link is crucial for the mitigation of adverse health outcomes. Here we present data from both experimental (patient-derived in vitro) and observational studies (a large population-based cohort) data confirming the link between AD and air pollution and showcase new mechanistic insight into this connection. We aimed to identify genetic and epigenetic changes in both healthy and AD individuals exposed to DE. Our approach included an in vitro model of patient-derived OM cells exposed to DE and subsequent miRNA, mRNA expression, and DNA methylation analyses. Moreover, we validated the in vitro findings with population-based data obtained from more than 2000 participants exposed to high- or low-level air pollutants. With this approach, for the first time, we expanded the data and findings obtained in a controlled laboratory experiment to data obtained in a large observational study. Using cutting-edge analysis, we successfully combined data and discovered new pathways and biomarkers valuable for (i) future AD research, (ii) research on the health effects of air pollutants, and (iii) research on the interplay between AD and air pollution. This comprehensive methodology and analysis enhance the understanding of air pollution's effects on health and AD.
2. **Interpretation**: The study findings contribute to the understanding of the heightened susceptibility of AD patients to the effects of air pollution exposure. The findings prove that AD cells exhibit a more pronounced response to DE, with key molecular pathways like oxidative stress, unfolded protein response, and ER stress being affected. Observed differential responses between AD and control cells on miRNA, mRNA, and methylome levels highlight the unique vulnerability of AD individuals to environmental stressors. The study also revealed unique DNA methylation patterns in AD OM cells, as well as differential methylation patterns in control and AD OM cell response to pollution exposure. These findings pave the way to future research into epigenetic regulation in neurodegenerative diseases and environmental biology. Additionally, by correlating in vitro data with population-based data, the study reinforces the importance of considering environmental factors in AD pathology. The work provides a great example of validation of in vitro data in population-based human cohort studies for increasing the translational potential of research and the successful identification of relevant systemic biological targets.
3. **Future directions**: Further investigation is warranted to validate and advance the discovery of air pollution exposure effects in both healthy and at-risk groups. Future studies may prioritize this aspect to enhance our understanding of pollution-related effects on the OM and the brain. Moreover, although our research has initiated the exploration and validation of defensive mechanisms employed by cells to counter adverse air pollution effects, more research efforts are needed to fully develop future mitigation technologies, such as antioxidant supplements or nasal sprays. Interventional studies targeting pathways like NRF2 might offer promising avenues to mitigate the effects of environmental pollutants in AD.

(iii) linking the data to the results from the in vitro cell exposures. This approach allowed us to validate our in vitro findings in a human cohort study and elucidate the main pathways involved in response to TRAP exposure.

2 | METHODS

2.1 | Cell culture model

Human OM biopsies were collected from cognitively intact (control) non-demented individuals and individuals diagnosed with AD (age-matched, female forty-eight samples in total were collected from eight donors). For all experiments, we used cells originating from four control and four AD donors that were divided into three individual replicates each for both treatment groups, resulting in 12 samples per group in the analysis. Each of the three individual replicates was exposed separately in 1 of the 3 weeks of the study exposure. Later, for the analysis, samples were combined, resulting in four analysis groups in total: control clean air, control DE, AD clean air, and AD DE. The OM biopsies were collected from the nasal septum, approximately 1 cm from the roof of the nasal cavity. Then primary OM cultures were established as described previously[13] with the ethical approval of the Research Ethics Committee of the Northern Savo Hospital District (permit number 536/2017). For ALI cultures, cells were seeded with a density of 150000 cells per insert. Twenty-four-well format Transwell cell culture inserts (Sigma-Aldrich, USA) were coated with Matrigel Growth Factor Reduced Basement Membrane Matrix (Corning, USA). Cells were cultured in a PneumaCult-ALI medium kit with hydrocortisone stock solution (both STEMCELL Technologies, USA), Heparin Solution (Parano LEO 5000 IU/mL), and Penicillin-Streptomycin (10,000 U/mL, Gibco, USA). The cells were grown in submerged conditions until a homogeneous culture was established (96 h), then medium was removed from the apical insert, while basal insert medium was changed daily.

After ALI culture was established, cells were grown at 37°C, 5% CO_2, and relative humidity > 90% in Transwell cell culture inserts (Sigma-Aldrich, USA). The cells were cultured at the ALI for 4 days before being subjected to exposure to either clean air or complete emissions.

2.2 | Exposure characteristics

DE was provided by a typical heavy-duty turbocharged six-cylinder, 6.5-L Iveco Tector diesel engine with common rail injection and no exhaust after treatment, running on ordinary on-road EN 590-compliant diesel fuel. The engine was coupled to a transient engine dynamometer and operated according to the 30-min World Harmonized Transient Cycle (WHTC) on 3 days, with one cold-start WHTC cycle, followed by one hot-start WHTC cycle, run each day. Complete DE was extracted from a full-flow dilution tunnel with an ALI exposure system described elsewhere[17,18] and used previously.[17,19]. One set of ALI cultures with OM cells was exposed to diluted DE (average particle mass concentration of 0.05 mg/m^3), and the second set, used as a reference, was exposed to synthetic air.

In short, ALI cultures with OM cells were exposed daily to either DE or fresh air for 1 h per day for 3 consecutive days. On the last day of exposure, cells and media were collected for analysis.

2.3 | Chemical analysis

Organic extracts/extractable organic matter gathered on filters at each exposure were extracted for chemical analysis using dichloromethane and cyclohexane and examined by high-performance liquid chromatography, as described previously.[20] Supplementary Material S1 reports comprehensive information on the collected particulate matter (PM), chemical analysis, and polycyclic aromatic hydrocarbon (PAH) concentration. Chemical analysis showed around 3% to 5.5% of carcinogenic PAHs in the sample. The most abandoned PAHs were phenanthrene, pyrene, and fluoranthene (Supplementary Material S1).

2.4 | Cell assays

The cytotoxic effects of air pollution were evaluated by lactate dehydrogenase (LDH) release in cell media using the CyQUANT LDH Cytotoxicity Assay Kit (Invitrogen, USA) according to the manufacturer's protocol. DNA damage was assessed with the DNA Damage Competitive ELISA Kit (Invitrogen, USA) that detects 8-hydroxy-2′-deoxyguanosine release in cell medium. Measurement was done according to the manufacturer's protocol. The human HSP70/HSPA1A DuoSet ELISA (R&D Systems, USA) was used for measuring heat shock protein 70 (HSP70) amounts in cell medium according to the manufacturer's manual.

2.5 | Transcriptome analysis

RNA and DNA were isolated with the AllPrep DNA/RNA/miRNA universal kit (QIAGEN, USA) according to the manufacturer's protocol. We used a Fragment Analyser System and RNA kit (15NT) for assessing RNA integrity numbers according to the producer's manual (Agilent Technologies, USA). The concentration of isolated RNA was measured with the Qubit RNA Hight Sensitivity (HS) Assay kit by the Qubit 4 fluorometer (Thermo Fisher Scientific, USA), and 200 ng of total RNA was used for mRNA selection with the NEBNext Poly(A) mRNA Magnetic Isolation Module (New England Biolabs, USA). mRNA libraries were prepared with NEBNext Ultra II Directional RNA Library Prep with Beads and NEBNext Multiplex Oligos for Illumina (all New England Biolabs, USA), and 100 ng of total RNA was used for miRNA library preparation with QIAseq miRNA Library Kit and QIAseq miRNA 96 Index IL (both QIAGEN). mRNA and miRNA libraries were assembled based on the manufacturer's instructions. The concentration of both types of libraries was checked with the 1× dsDNA HS kit (Thermo Fisher Scientific, USA) on the Qubit 4 fluorometer, and their profile and size were analyzed by the Fragment Analyzer with the HS NGS Fragment Kit (both Agilent Technologies, USA). mRNA libraries were pair-end sequenced (2 × 60 cycles) using NovaSeq 6000 S1 Reagent Kit version 1.5 (100 cycles), and miRNA libraries were single-end sequenced (85 cycles) using NovaSeq 6000 SP Reagent Kit version 1.5 (100 cycles) (all Illumina, USA).

As samples were sequenced into two separate lanes, the FASTQ format reading resulting from the same sample was concatenated. Reads were aligned using STAR (version 2.7.9)[21] to the GRCh38 human reference genome, indexed through a GTF annotation file retrieved from GENCODE (version 41). The quantMode GeneCounts option in STAR was used to obtain a count table from mapped reads. Quality control of raw and aligned reads was performed using FASTQC (version 0.11.9). Downstream statistical analyses were carried out using the R packages edgeR (version 3.38.2)[22] and limma (version 3.52.2)[23] from the Bioconductor framework. Genes having low expression (count < 15) in more than 12 samples, the cardinality of each experimental condition, were filtered out. The normalization coefficients were computed using the trimmed mean of M-values (TMM) method. Multidimensional scaling was performed to identify potential sources of variation in the dataset related to experimental conditions of interest and other conditions (cell line, replicates, smoking habits, hyposmia). For the within-control (control DE exposed vs control clean air) and within-AD comparison (AD DE exposed vs AD clean air) the samples were paired by cell line and replicated to reduce unwanted variation. In the between-control and AD contrast (AD clean air vs control clean air), the only source of external variation considered was smoking habits, which was included as a covariate in the model. The voomWithQualityWeights function with cyclic loess normalization was used to compute gene weights. A linear model was fitted using lmFit, and standard errors were smoothed with empirical Bayes. Significant DEGs for each contrast were defined as genes with adjusted p value < 0.05 calculated with the default Benjamini–Hochberg method, and functional analysis was performed on them. Gene Ontology enrichment analysis was accomplished using the clusterProfiler R package (version 4.4.4).[24] Ingenuity Pathway Analysis (IPA)[25] was used to identify canonical pathways and transcription factors significantly altered in each condition. miRNA differential expression workflow was the same as that of transcriptomic data. miRNA targets were detected with the miRNAtap R package (version 0.99.10),[26] which collects annotated targets from the five most commonly cited databases: miRDB,[27] DIANA,[28,29] TargetScan,[30] PicTar,[31] and Miranda.[32–34] We selected for analysis miRNA that had been annotated in a minimum of two databases.

2.6 | Whole-genome DNA methylation analysis

First, the combination of genomic DNA (200 ng) and control DNA was fragmented to an average insert size of 240 to 290 bp on a Covaris ME220 (duration 95 s, peak power 75 W, duty factor 25%, cycles per burst 1000, temperature 20°C) (Covaris, LLC, USA). Libraries were prepared with a NEBNext Enzymatic MethylSeq kit according to the manufacturer´s instructions (New England Biolabs, USA). DNA sequencing was performed on an Illumina NovaSeq 6000 with 2 × 160 base read using a NovaSeq 6000 S4 Reagent Kit (all Illumina, USA). The FASTQ paired-end methylation files that resulted from whole-genome sequencing were processed with an nf-core/methylseq pipeline (version 1.6.1). The resulting bsseq files were transformed into tab-separated text files, with expected input of the methylKit R package. MethylKit was used to perform differential methylation analysis at the base level. The methylated bases were mapped with ChIPpeakAnno to genomic regions as defined by TxDb.Hsapiens.UCSC.hg38.knownGene to determine their location with respect to genes. Additionally, a differential analysis on predefined regions was performed, namely, of gene bodies, promoter regions (defined as 1.5 kb upstream and 5 kb downstream from transcription start sites), and mature miRNA sequences (mirbase version 22) to link methylation levels to the relative differential expression of miRNA and mRNA.

2.7 | Validation of identified DEGs in class-specific pathways from Rotterdam Study

We used Patient Similarity Network analysis to identify class-specific features of individuals who develop dementia during follow-up and compared those to features of dementia-free controls. In addition, data on exposure to air pollution were used to perform a classification task between participants living in areas with different levels of pollution in order to determine features that are common to participants living in highly polluted areas compared to less polluted areas. We sought data from the ongoing prospective population-based Rotterdam Study that started in 1990 with 7983 participants aged 55 years and older (78% of the invitees).[35] At study entry and subsequently every 3 to 4 years, all participants were invited to undergo extensive examinations. Between 2002 and 2004, corresponding to the fourth examination round (RS-I-4), plasma samples were collected from 2657 participants (74.8% of the surviving participants) and included in the analyses of the current study. The majority of participants in our study were of Caucasian origin, which may limit the generalizability of our findings.

2.7.1 | Data collection

AD

Participants were screened for dementia at baseline and every 3 to 6 years during follow-up examinations using the Mini-Mental State Examination (MMSE) and the Geriatric Mental Schedule (GMS) organic level. Those with a MMSE score of <26 or a GMS organic level score over 0 were further examined using the Cambridge Examination for Mental Disorders in the Elderly diagnostic interview. Participants were also monitored for dementia continuously through an electronic link between the study database and medical records from general practitioners and the Regional Institute of Outpatients Mental Health Care. The final diagnosis was established by a consensus panel led by a neurologist, according to standard criteria for AD (National Institute of Neurological and Communicative Diseases and Stroke/Alzheimer's Disease and Related Disorders Association).

General and clinical characteristics

During home interviews, information was obtained on age, sex, educational attainment (classified as primary, lower, intermediate, or higher), and smoking status (classified as current, former, or never). During these same home interviews, data on the use of blood pressure-lowering, lipid-lowering, and glucose-lowering medication were obtained. Waist circumference in centimeters was determined at the research center. Systolic and diastolic blood pressure (mmHg) was measured twice on the right arm with the participant in a sitting position using a random zero sphygmomanometer and averaged. Apolipoprotein E (*APOE*) genotype was obtained using a polymerase chain reaction of coded DNA samples.

Air pollution

Exposure to air pollution was calculated at participants' geocoded residential addresses using land use regression models, as described in detail elsewhere.[36] Modeled air pollutant concentrations included PM of less than 10 μm (PM10) and 2.5 μm (PM2.5) in diameter, a proxy of elemental carbon (PM2.5 absorbance), nitrogen oxide (NO_x), and nitrogen dioxide (NO_2).

Metabolite profiling

Fasting plasma samples from participants were collected in EDTA-coated tubes and utilized to quantify metabolites using 1H-NMR technology. A comprehensive array of metabolites, including amino acids, glycolysis-related metabolites, ketone bodies, fatty acids, routine lipids, and lipoprotein subclasses, was simultaneously quantified using the Nightingale Health metabolomics platform (Helsinki, Finland). Details on the method can be found elsewhere.[37]

Genotype profiling

At the study entry, whole blood samples were collected for the subsequent extraction of genomic DNA as described in detail elsewhere.[38] Briefly, the salting-out method was employed for this purpose. Microarray genotyping was performed using the Infinium II HumanHap550K Genotyping BeadChip version 3 (Illumina, USA). Genotyping procedures were followed according to the manufacturer's protocols.

Data preprocessing

Overall, 231 metabolites were assessed, which were classified into 42 functional groups, as adapted from Nightingale Health's grouping of metabolites (https://research.nightingalehealth.com/biomarkers). Metabolites with more than 20% missing values were removed. Missing values on other metabolites were imputed to half the minimum for that metabolite across samples.[39]

Genotype data were preprocessed as follows. Plink (version 1.9)[40] was used for quality control (–mind 0.01, –geno 0.05, –maf 0.05). A binary matrix was built where rows corresponded to genes and columns to samples. We assigned a value of 1 to samples with any common variant in the gene and a value of 0 to those without. Then the matrix was filtered to retain only genes that might be relevant for classification by performing common variant association analysis with the disease phenotype. Specifically, common variants analysis was performed using a model based on region association analysis.[41] In region association analysis, common variants are grouped into sets based on their genomic location, such that common variants in the same gene are considered as a single set. Association of common variant sets in comparison to participants with AD and controls were performed to identify genes linked to the disease phenotype. Finally, the binary matrix was split into submatrices, representing pathways of interest, so as to obtain a binary matrix of the genes belonging to each pathway. Biological pathways were retrieved from Enrichment Map Gene Sets,[42] which were compiled from multiple curated pathway databases (version April 2022), filtered to exclude pathways having less than 10 or more than 200 genes and composed of at least one gene with differential common variant coverage, resulting in 656 biological pathways.

Common variants, despite their modest individual effects, play a significant role in explaining polygenic diseases like AD. Genome-wide association studies (GWAS) have identified numerous common variants associated with AD, underscoring their importance in the disease pathogenesis.[41,43–45] Being more prevalent, common variants are more likely to show significant interactions with environmental influences. Therefore, by employing data from the Rotterdam Study cohort, we performed an analysis of common variants to better understand the interplay between air pollution and AD-related pathways.

For each data feature we obtained after preprocessing (12 clinical features, 42 metabolite groups, and 656 biological pathways), a similarity matrix was created, indicating a similarity between samples for each feature, thereby creating 710 patient similarity networks (PSNs). That is, we used normalized difference for continuous variables (age, waist diameter, pressure, pulse) and categorical ordinal variables (education) after having encoded the values on a numeric scale, and we used average normalized difference for matrices of continuous variables (metabolites); for binary variables, similarity was positive on belonging to the same category (smoking, medications, *APOE* genotype), and for a binary variant matrix, similarity was positive for pathways having at least one common variant in both samples.

Classification

During follow-up, 383 participants developed dementia. The classification was conducted on a down-sampled dataset, such that the controls were randomly chosen in the pool of samples to perform a balanced analysis (a total of 766 samples of which 383 had AD and 383 were controls). The training set corresponded to 80% of the down-sampled dataset, the rest being used as a test set.

PSNs are the input of patients' classifiers. For classification, we use the R package netDx,[46,47] which is a network-based patient classifier that uses the concept of PSNs to integrate several sources of information into a network, where nodes are patients and edges reflect their similarity. The tool learns features that are specific to each class and uses this information to classify unlabeled samples to the class that more closely resembles them. Binary classification was performed between the classes of incident disease (AD) and controls. The parameters of the buildPredictor function from netDx are the following: numSplits = 100, featScoreMax = 10L, trainProp = 0.8, featSelCutoff = 9L. The significant features detected in the training run are used to classify the test set of samples and validate the predictivity of the features.

Additionally, we used pollution levels at the participants' geocoded residential addresses to perform a classification task based on the separation of the population into two classes corresponding to higher (HI) and lower (LO) levels of pollution. We included only controls to determine the features linked to pollution exclusively and avoid confounding with effects of AD. The separation was achieved using *k*-means clustering ($k = 2$) on the lower-dimensional representation of the first two principal components of the five air pollutants, explaining 93.6% of the variance. The smaller class (HI) contained 70 samples, so we down-sampled the LO group to create a balanced dataset, obtaining a total of 140 samples. Other features used in this setting were the same as those described in earlier sections, but in this case, 551 biological pathways resulted from the initial preprocessing.

Significance testing

Overlap between deregulated genes in transcriptomic analysis and significant pathways in the population-based Rotterdam Study was computed by counting the number of pathways containing deregulated genes and being significant in the Rotterdam Study. Significance was assessed by randomly subsampling the full set of genes used to perform transcriptomic analysis 1000 times and computing the overlap with genes in AD-specific pathways. The empirical *p* value was obtained as the number of times the random sets of genes resulted in an equal or higher number of overlapping pathways than what was observed with the true set of deregulated genes.

3 | RESULTS

3.1 | Transcriptomic data

miRNA and mRNA expression was determined in exposed OM cells by sequencing in the following experimental groups: control clean air, AD clean air, control DE exposed, and AD DE exposed. Only genes with adjusted *p* values < 0.05 were reported for every comparison.

Before assessing the effects of DE exposure on the OM cell model, we first quantified changes in mRNA expression between the control and AD ALI cultures in the clean-air groups to determine solely the effect of existing AD pathology on the gene expression profiles. When comparing clean-air controls originating from AD individuals, the AD clean air group, against cognitively unimpaired individuals, the control clean air group, we found 483 differentially expressed mRNAs. For

additional evaluation of the AD-related phenotype in this cell model, we computed the retrieval of a network of interactions between the DEGs and AD markers using the IPA software. In the list of DEGs for the comparison of "AD clean air" versus "control clean air," 76 genes directly associated with AD were found. Among these AD-associated genes, 47 were deregulated in our dataset, and the deregulation of 29 more genes was calculated by IPA (Figure S1). *HSPA1*, *NQO1*, *HMOX1*, *PLAU*, *SNRNP70*, *CDC42EP3*, *SQSTM1*, *XBP1*, and *UCHL1* were among the deregulated genes in the AD OM cells, which were also previously reported to be altered in AD.[48–52] These data confirm our previously published findings that OM cells from AD individuals maintain a disease-related phenotype in culture[13,14] and that this cell model is suitable for preclinical research.[12] The detailed pathway analysis is presented in Supplementary Material (Figure S1).

To quantify the response of both control and AD cells to DE exposure, initially we aimed to assess whether the exposure design induced any significant toxic responses. Cytotoxicity was assessed in the clean air control and DE-exposed samples from the cell culture medium using the LDH release assay and DNA Damage ELISA kit 3 days after exposure at ALI. No exposure-induced or genotype-specific changes in LDH and 8-hydroxy-2′-deoxyguanosine release were detected by two-way ANOVA in OM cells derived from control donors or individuals with AD (Figure S2).

When mRNA expression was assessed, we detected a robust change in transcriptomic responses. Strikingly, in accordance with our hypothesis, AD cells were more susceptible to DE exposure than cells derived from healthy controls, with four times higher numbers of DEGs detected. In cells originating from cognitively unimpaired individuals, a total of 161 significant DEGs were detected when clean air control was compared with DE-exposed cells. Among those genes, 79 DEGs were significantly upregulated after exposure, and 82 were downregulated (adj. p value < 0.05) (Supplementary Material S2). In AD cells, 585 DEGs were detected when DE-exposed cells were compared to the clean air control. A total of 287 DEGs were significantly upregulated in AD DE-exposed cells, and 298 were downregulated (adj. p value < 0.05) (Supplementary Material S2). The numbers of unique and common significantly altered DEGs after DE exposure in both control and AD cells are presented in Figure 1A. Among common significant DEGs in both AD and control cells after exposure, we found heat shock protein Family A (Hsp70) Member 6 (*HSPA6*) to be highly upregulated. Additionally, *HSPA1A* from the same family of HSPs was activated in both control and AD cells after exposure. Heme oxygenase 1 (*HMOX1*) and glutamate-cysteine ligase modifier subunit (GCLM) proteins had the second-highest expression values (Figure 1A). Both genes were previously reported to be involved in the oxidative stress response in both healthy and AD cells.[54,55] In both AD and control cells, a group of the top common upregulated genes induced by exposure were either oxidative stress response genes or members of HSPs.

Among the downregulated genes in DE-exposed control cells, we found macrophage-stimulating protein (*MST1*, logFC −0.5) and C-X-C motif chemokine ligand 1, a chemokine that is involved in inflammation and acts as a chemoattractant for neutrophils (*CXCL1*, logFC −0.25) (Supplementary Material S2).

In AD cells, the Fos gene family member *FOSB* was highly downregulated after DE exposure (logFC −2.77) (Figure 1B, Supplementary Material S2). *FOSB* was previously found to be deregulated in lung cells after PM10 exposure.[56] In addition, nuclear receptor subfamily 4 group A (*NR4A*) genes were highly downregulated in AD cells after DE exposure. The NR4A family consists of three members: NR4A Member 1 (*NR4A1*, logFC −1.86 in AD DE-exposed cells), *NR4A2 (*logFC −1.68 in AD DE-exposed cells), and *NR4A3 (*logFC −0.92 in AD DE-exposed cells) (Figure 1B, Supplementary Material S2), all of which were downregulated.

Oxidative stress induction is a commonly reported cellular consequence of exposure to air pollution that is described in a variety of models. Therefore, we evaluated whether DE exposure at ALI could cause the induction of oxidative stress genes also in the unique human OM cells. In total, we found 13 oxidative stress-related genes deregulated in control cells after DE exposure and 18 deregulated oxidative stress-related genes in AD-exposed cells (Figure 2). Genes were considered related to oxidative stress response if they were annotated as part of either the biological process "response to oxidative stress" (GO:0006979) or "cellular response to oxidative stress" (GO:0034599). Our data showed that the oxidative stress pathway was deregulated by both mRNAs and miRNAs in the AD cells.

3.1.1 | Integration of mRNA and miRNA expression

We additionally performed an analysis of miRNA expression values in exposed cells and analyzed the correlation between mRNA and miRNA expression values. Differential expression miRNA values for each analyzed group are presented in Supplementary S3. Some miRNAs that are altered after DE exposure in our data were previously reported to be deregulated in AD. In control cells, miR-1200, miR-514b-3p, and miR-340-5p were deregulated after DE exposure (Supplementary Material S3) and were previously reported as either biomarkers of AD or to be deregulated in AD.[57,58] Additionally, three top upregulated miRNAs, miR-601, miR-1197, and miR-591, in DE-exposed control cells were previously identified as tumor suppressors.[59–61] Notably, miR-4281, which is upregulated in DE-exposed control cells, was previously reported to be similarly upregulated after exposure of lung cells to aldehydes, which are present in pollutants.[62] We propose that this miRNA is implicated in both OM and nasal cells; however, the exact pathways that it activates require further investigation.

For the integration of mRNA and miRNA expression values, we integrated differential miRNAs and mRNAs in each group for verifying the detected expression patterns and finding common components involved. A full list of differentially expressed targets of differential miRNAs is in Supplementary S3. Notably, we found some miRNAs, namely, miR-663a, miR-4792, and miR-508-5p, to be inversely correlated with their target genes related to oxidative stress response in the AD DE-exposed group (Figure 3).

In DE-exposed control cells, there were also two miRNAs, miR-6828-5p and miR-1197, with an inverse correlation to the expression of their oxidative stress-related target genes. We further identified

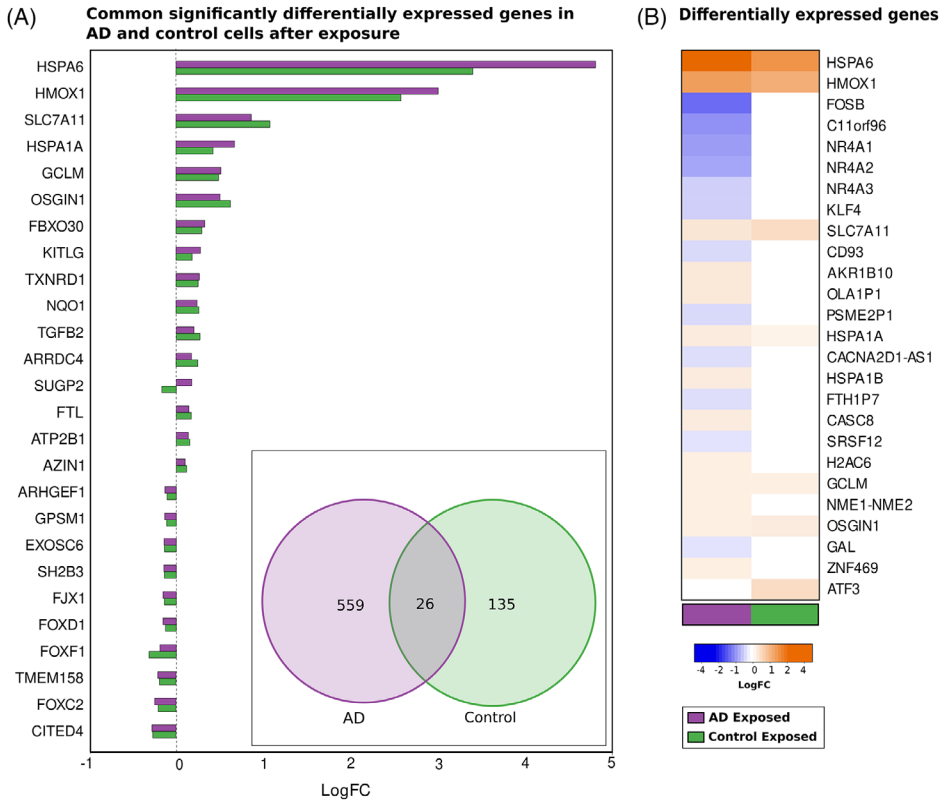

FIGURE 1 Transcriptomic changes in control and AD OM cells caused by DE exposure. Common and top deregulated genes. (A) List of common significant DEGs in both control and AD cells after DE exposure (p-adjusted < 0.05) sorted by decreasing logFC. Venn diagram showing number of DEGs in AD and control cells after exposure. (B) Heatmap showing expression value for most deregulated genes (highest absolute logFC value) after DE exposure (p-adjusted < 0.05). AD, Alzheimer's disease; DE, diesel emissions; DEG, differentially expressed gene.

target genes involved in unfolded protein response (UPR) in both control and AD DE-exposed groups with an inverse correlation to their regulating miRNA, miR-601 regulating HSPA6 and HSPH1 in control exposed cells, and miR-1246 and miR-663a in AD exposed cells.

3.2 | Pathway analysis

3.2.1 | Canonical pathways

We found a striking difference between the control and AD cell responses to DE exposure in our pathway analysis. Among significantly activated pathways after DE exposure in control cells, we found only the nuclear factor erythroid 2–related factor 2 (NRF2)-mediated oxidative stress response pathway (Figure S3) and xenobiotic metabolism to be activated. Activation of NRF2 and xenobiotic metabolism signaling pathways indicates activation of the protective cell defense system in control cells, which includes drug-metabolizing enzymes, xenobiotic transporters, and antioxidant enzymes. Xenobiotic metabolizing enzymes play a crucial role in the biotransformation, metabolism, and detoxification of xenobiotics, including various types of pollutants, to protect cells against potential harmful insults from the environment. For the AD cells, the number of pathways altered by DE exposure was significantly higher (Figure 4A).

3.2.2 | Upstream regulators

When top significant upstream regulators were assessed, we observed significant activation values for *NFE2L2*, the gene encoding the NRF2 transcription factor, in both control and AD cells after exposure. This confirms the key role of the NRF2 antioxidative stress response as a defense mechanism activated in OM cells after air pollution exposure (Figure 4B). Additionally, we assessed the downstream targets of the NRF2 transcription factor and found a great variety of genes to be upregulated in both control and AD cells after exposure (Figure 4C). The second most activated upstream regulator in AD cells after *NFE2L2* was N-acylsphingosine amidohydrolase responsible for ceramide breakdown – *ASAH1* (Figure 4B).

3.2.3 | Unfolded protein response pathway is highly attenuated (and thus upregulated) in AD cells

Cells regulate the protein homeostasis of the endoplasmic reticulum (ER) through the UPR. The UPR is not activated under normal conditions, but under stress conditions it can become activated due to an accumulation of unfolded proteins. *HSP70*, a chaperone, acts as an important member of the UPR pathway and was found to be highly upregulated only in AD cells after DE exposure at ALI (Figures 4A, 5).

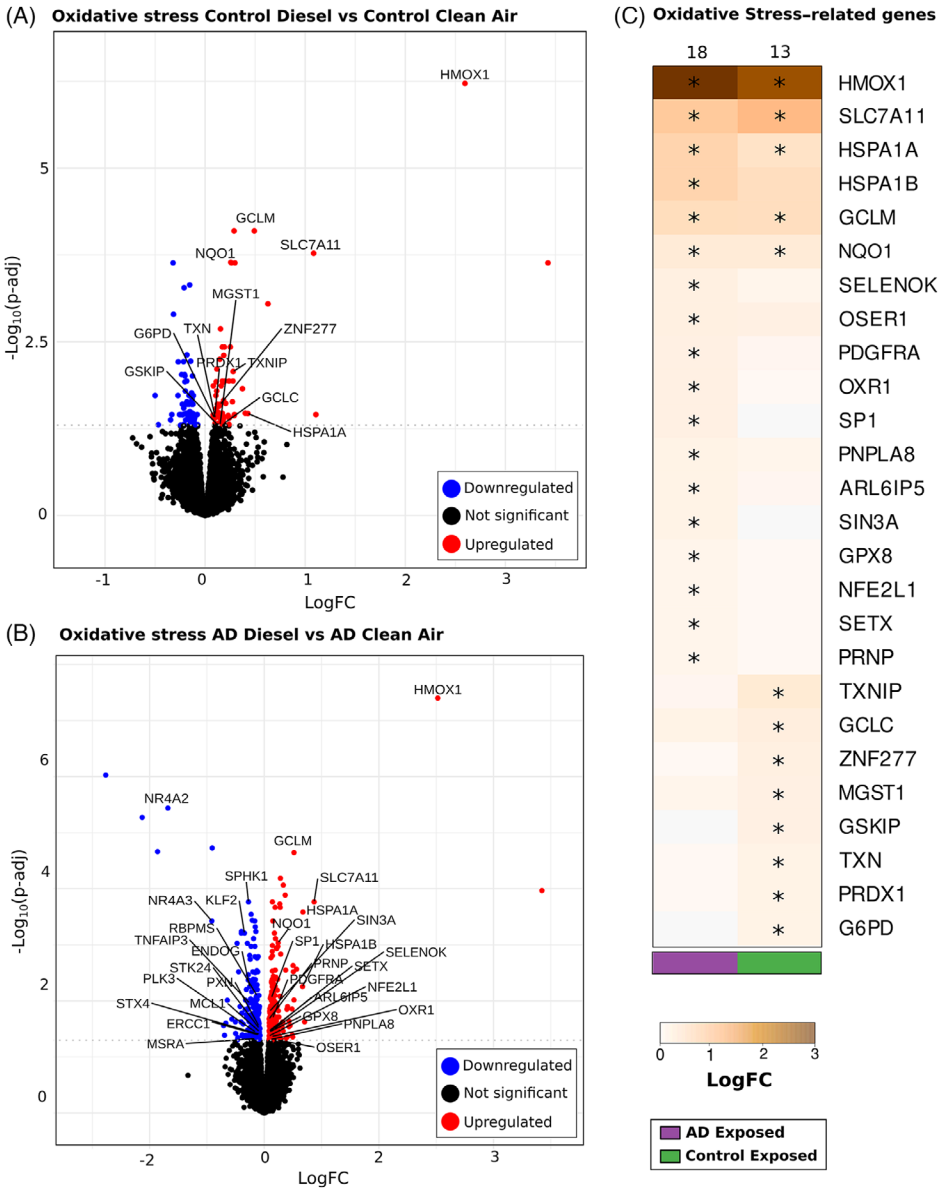

FIGURE 2 Induction of oxidative stress response in control and AD OM cells after DE exposure. Volcano plot highlighting the most altered oxidative stress genes after DE exposure in control (A) and AD (B) OM cells. Here, we labeled on the plot genes that were previously reported in a Gene Ontology biological process related to oxidative stress. The *y*-axis of the volcano graph is -log10 (*p* value), the *x*-axis is the logFC value; red: upregulated genes, blue: downregulated genes. (C) Heatmap of top-upregulated oxidative stress-related genes induced by DE exposure in AD cells (left) and control cells (right). The asterisk indicates the genes significant in the category. On top is indicated the number of significant genes that cause an enrichment in oxidative stress. AD, Alzheimer's disease; DE, diesel emissions; OM, olfactory mucosa.

Additionally, heat shock protein Family A (Hsp70) Member 6 (HSPA6), a component of UPR pathway, was found to be highly upregulated in DE-exposed AD cells (Figure 1). These results suggest that the UPR pathway is deregulated on both mRNA and miRNA levels. Similarly, the BAG2 pathway, which shares several common proteins with the UPR pathway, was found to be highly activated in DE-exposed AD cells (Figure S4). The ER stress pathway, which is a component and activator of UPR, was also found to be activated in DE-exposed AD cells (Figure S5).

We hypothesized that *HSP70* induction in exposed cells can be part of the cellular protective mechanism against pathological processes induced by exposure, such as the aggregation of unfolded proteins. Therefore, we sought to quantify HSP70 protein release from exposed cells. A significant increase in the concentration of HSP70 in cell media was found after exposure in AD but not in control cells (Figure 6A).

Lastly, we assessed possible predictive/prognostic functional markers, such as smell loss (anosmia), and morphological markers, such as abnormal olfactory epithelium morphology, in our data. For this prediction analysis, we conducted the retrieval of a network of interactions between our DEG list of contrast (control DE vs. control air, AD DE vs. AD air) and markers of anosmia or markers of abnormal morphology of the olfactory epithelium using IPA software. When we assessed

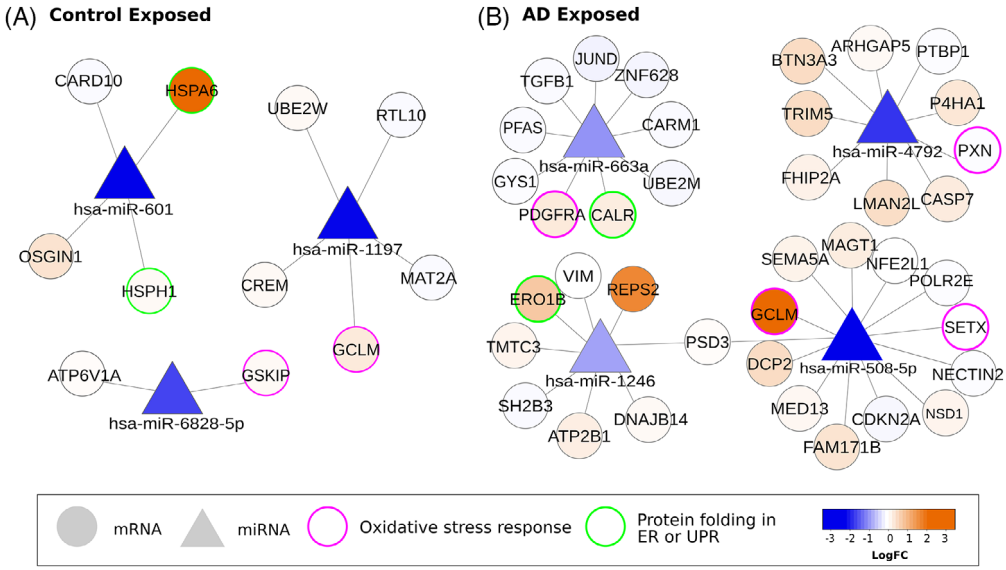

FIGURE 3 Differentially expressed miRNA–mRNA relationships in (A) control and (B) AD OM cells after DE exposure. Specifically, the anticorrelated relationships between miRNA and genes of some relevant pathways are depicted. Pathways investigated relate to oxidative stress response (GO:0006979 and GO:0034599) and response to unfolded protein or protein folding in the ER (GO:006986 and GO:0034975). The color scale corresponds to the logFC expression of miRNA and mRNA, the triangle-shaped nodes represent miRNA, while circles are mRNAs. Colored borders of nodes indicate the target genes involved in the respective pathways. AD, Alzheimer's disease; DE, diesel emissions; ER, endoplasmic reticulum; OM, olfactory mucosa.

whether DE exposure might be associated with markers of anosmia, we found only two genes (*Slc7A11* and *BACH1*) involved in smell loss according to IPA annotation and deregulated by DE exposure in control cells (Figure S6). When markers of an abnormal morphology of epithelial tissue were assessed, 14 genes that are affected by exposure in control cells were found to be associated to this condition (Figure S7). This result should be interpreted with caution since most of those 14 genes are also implicated in a wide variety of cellular pathways. In contrast to control cells, when the same analysis was performed in AD cells, exposure resulted in differential expression of 21 genes associated with anosmia (Figure S8). We also detected 48 genes, like *TGFB1*, *CYLD*, *REL*, *NFATC2*, *BCL3*, *E2F4*, and others, to be deregulated after exposure, and three genes predicted to be affected among markers of abnormal epithelial tissue morphology in DE-exposed AD cells (Supplementary Figure S9). These provide prediction markers that can be potentially assessed in real-life exposures and support the hypothesis that AD patients are an at-risk group for adverse air pollution exposure effects.

3.3 | DNA methylation and DMR–DEG correlation

Epigenetic modifications can govern gene expression without altering the DNA sequence and therefore may react rapidly to environmental changes. One of the main epigenetic alterations, DNA methylation, is crucial for the control of gene expression as well as for the stabilization of genome and chromatin modification.[63] Alterations in the DNA methylation profile have been detected after air pollutant exposures in human blood and lung samples,[64] and patterns of DNA methylation are attenuated in several diseases, representing a promising target for biomonitoring and identification of prognosis markers.[65] Only a few studies currently exist that attempted to estimate the effects of air pollution on both transcriptome and DNA methylome profiles.[66,67] Here, we aimed to identify DNA methylation sites that are altered by DE exposure and to find a correlation between methylation profiles and mRNA expression. DNA methylation, especially within gene promoters, CpG islands, and gene bodies, is associated with changes in gene expression. We first assessed methylation levels for different positions and regions in the genome. We made pair-wise comparisons for the groups AD clean air versus control clean air, control DE exposed versus control clean air, and AD DE exposed versus AD clean air. The comparison is presented as differentially methylated positions (DMPs) and regions (DMRs). Overall, 262933 DMPs were found when the AD clean air group was compared with control clean air cells. 15222 DMRs were found in the gene body: 14090 with positive methylation differences (hypermethylation), 1132 with negative methylation differences (hypomethylation), and 9586 DMRs with methylation in the promoter region. When we compared control DE exposed cells with the control clean air group, we found 21 DMPs, 5212 DMRs in the gene body (3754 with positive methylation difference and 1458 with negative), and 890 DMRs in promoter regions. For AD cells, DE exposure resulted in 13 DMPs, 5659 DMRs in the gene body (2097 with positive methylation difference and 3562 with negative) (Supplementary Material S4), and 1088 DMRs in promoter regions. Notably, while in control cells more genes were hypermethylated after exposure, in DE-exposed AD cells we observed slightly higher amounts of hypomethylated genes.

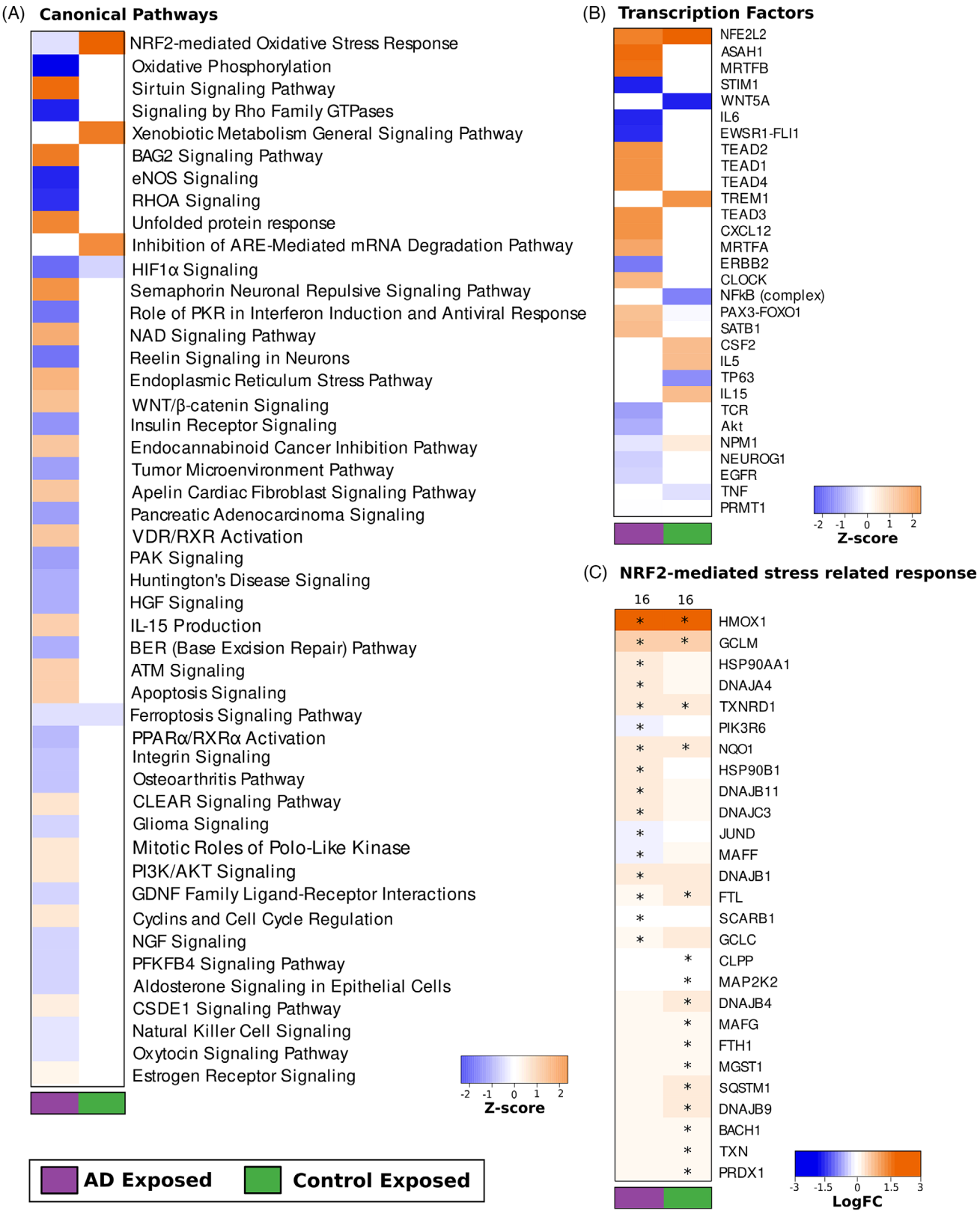

FIGURE 4 (A) Top canonical pathways activated by DE exposure in OM cells provided by IPA software, sorted by z-score value. (B) Top significant transcription factors, sorted by activation value (z-score). (C) Heatmap showing NRF2-mediated oxidative stress response genes affected by DE exposure in control and AD OM cells. The asterisk indicates the genes significant in the category and that were used in the enrichment. On top is indicated the number of significant genes that cause an enrichment in oxidative stress. AD, Alzheimer's disease; DE, diesel emissions; IPA, Ingenuity Pathway Analysis; NRF2, nuclear factor erythroid 2–related factor 2; OM, olfactory mucosa.

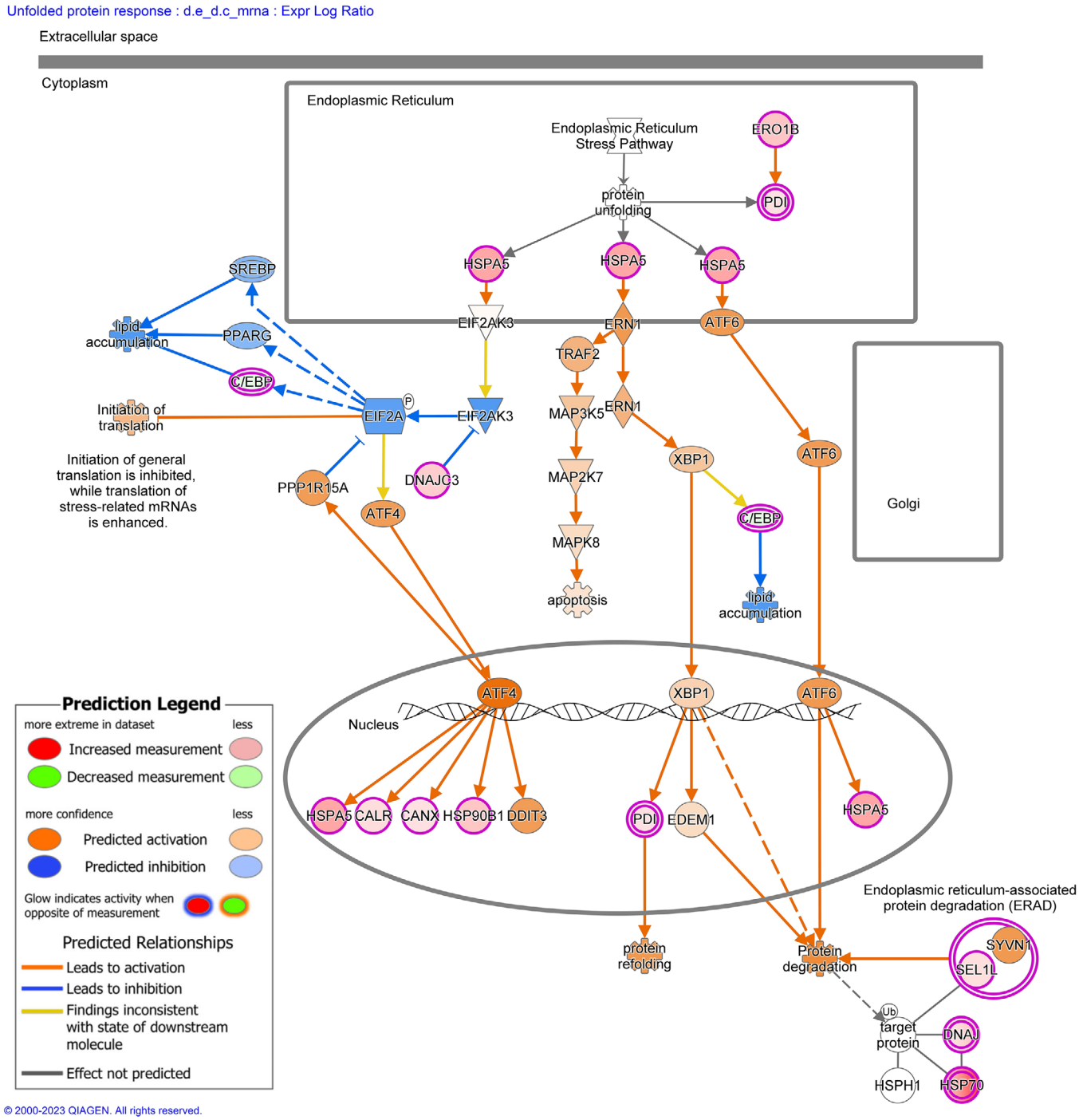

FIGURE 5 Activation of UPR pathway in AD OM cells after DE exposure calculated with IPA software. AD, Alzheimer's disease; DE, diesel emissions; IPA, Ingenuity Pathway Analysis; OM, olfactory mucosa; UPR, unfolded protein response.

To investigate how methylation affected mRNA expression in our study, we integrated the methylomes and transcriptomes obtained. Overall, 352 DEGs were found for the comparison between the clean air AD and control groups, among which 12 DEGs were hypomethylated and upregulated in AD, while 164 were hypermethylated and downregulated in AD (Figure S10). In the control group, 41 DEGs were found in comparisons of DE-exposed cells with clean air controls. Only three of those genes were hypomethylated and upregulated, and 16 were hypermethylated and downregulated, including the *FOXF1* gene (Figure 6C). In AD cells, we found 165 DEGs where methylation data were intersected with mRNA expression data for the comparison of DE-exposed AD cells versus clean air AD. Fifty genes were found to be both hypomethylated and upregulated, and 25 genes were hypermethylated and downregulated, including the highly downregulated gene *N4A2* (logFC −1.68) (Figure 6D).

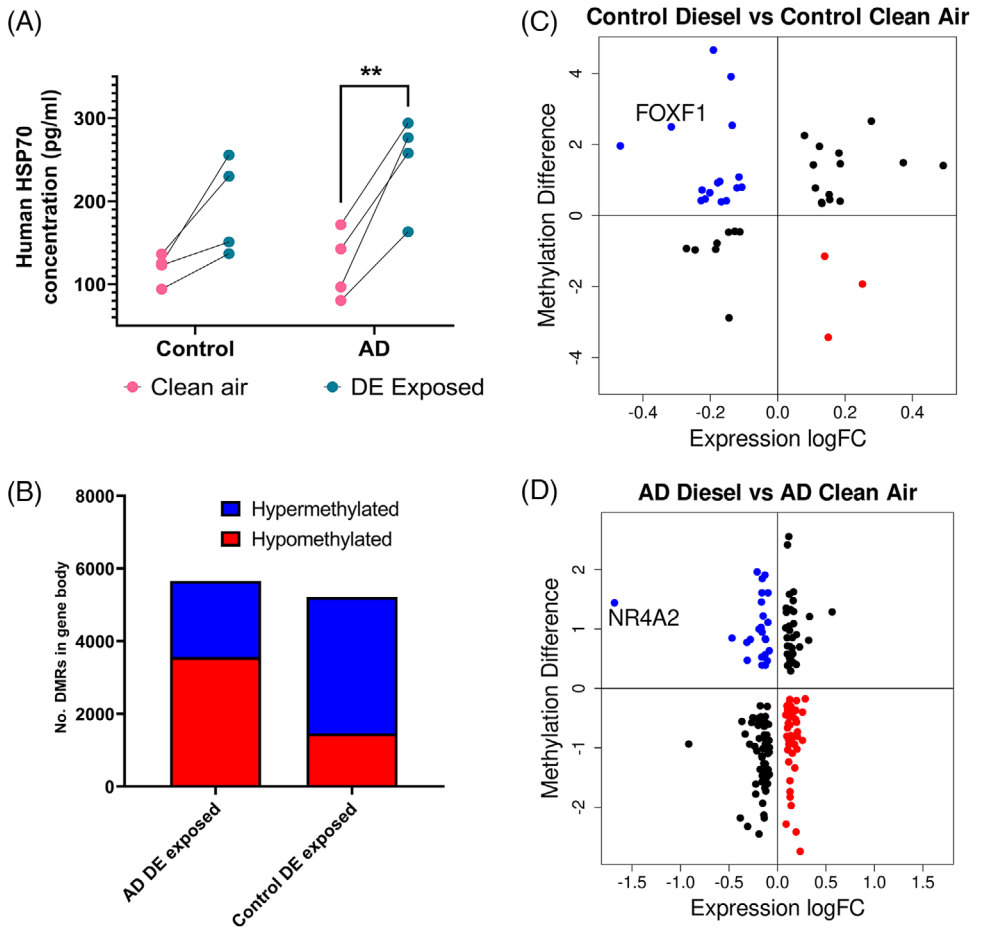

FIGURE 6 (A) HSP70 level is increased in AD OM cell media after DE exposure. Quantification of HSP70 was performed with ELISA and *t*-test (unpaired, two-tailed, two-way ANOVA with Sidak multiple test). Data are presented as mean ± SD, $^{**}p < .01$. (B) Graphical representation of number of DMRs and relative methylation change (hyper vs hypo) after DE exposure in control and AD OM cells. Figures represent correlation of DMRs with mRNA expressions altered in control OM cells (C) and AD OM cells (D) after DE exposure. AD, Alzheimer's disease; DE, diesel emissions; DMR, differentially methylated region; HSP70, heat shock protein 70; IPA, Ingenuity Pathway Analysis; OM, olfactory mucosa.

3.4 | Validation of identified DEGs in class-specific pathways from Rotterdam Study

The main tasks performed in the Rotterdam Study aimed to (i) identify biomarkers that were differential in AD compared to controls, (ii) link the identified biomarkers to differential air pollution data in the Rotterdam Study, and (iii) link the Rotterdam data to the results from the OM cell exposures. This approach allowed us to validate our in vitro findings in a human population-based study and elucidate the main pathways involved in response to air pollution exposure in both control and AD individuals.

First, we classified patients between the samples belonging into classes of AD and controls based on disease incidence, obtaining an area under the receiver operating characteristic (AUROC) of 0.79. The analysis resulted in 115 features that were significant in predicting AD (listed in Supplementary Material S5, AD Significant Features), including three clinical features (*APOE* ε4 carrier, diabetes, education level) and 112 biological pathways. A full list of identified pathways is presented in Supplementary Material S5. Then we compared 112 biological pathways that were found to be class-specific by netDx in AD participants from the Rotterdam Study with the genes identified in non-exposed AD OM cells and detected similarities. For example, pathways like amino acid transport, xenobiotic metabolism, inflammatory response, NRF2 pathway, and respiratory electron transport were found to be AD-specific features in the Rotterdam Study. Similarly, genes that are part of these pathways were deregulated in non-exposed OM cells obtained from AD individuals (Supplementary Material S5). Some of these pathways and genes that we found in our analysis may provide important insights for future AD research. For example, we found pathways like amino acid transport across the plasma membrane to be predictive in AD participants from the Rotterdam Study, with *SLC38A5* and *SLC38A1* genes in this pathway to be deregulated in AD OM cells in our study. Similarly, we found pathways like cytoprotection by HMOX1 (genes *HELZ2*, *STAP2*, *LRPPRC*), apoptosis (*HGF*, *ANKH*), inflammatory response (*PTGER4*, *TNFRSF1B*, *LYN*, *HRH1*, *IL1R1*), xenobiotic metabolism (*AKR1C2*, *NPC1*, *DHRS1*, *IL1R1*, *MAN1A1*, *PMM1*, *ACOX3*, *LONP1*), fatty acid metabolism (AKR1C3, PRKAA2, CYP2U1, ACOX3, MMUT), and many others to be significantly deregulated in

both in vitro AD cells and class-specific AD individuals from the Rotterdam Study (Supplementary Material S5, AD Significant Features).

We then compared the AD-specific pathways that were identified from the Rotterdam Study with the genes that were deregulated by DE exposure in the OM cells in vitro. We found that genes deregulated by DE exposure in the AD-exposed OM cells were represented in AD-specific pathways more often than what would be expected by chance (p value < 0.05, median fold change 1.163). Overall, we found a larger number of pathways with DEGs in AD-exposed cells than in control cells (93 vs 52). Almost all pathways found in controls were included in the AD-exposed list, indicating greater dysregulation in DE-exposed AD OM cells, linking them to the AD-specific pathways found in the Rotterdam Study. Among AD-specific pathways containing DEGs from DE-exposed AD OM cells, we found pathways related to apoptosis and caspase-mediated cleavage (genes *CASP7*, *ROCK1*, *STK24*, *VIM*, *HMOX1*, *ISG20*, *DNAJC3*, *RNASEL*, *TNFRSF12A*, *ROCK1*, *CYLD*, *MCL1*, *IGF2R*), cytoprotection by HMOX1 (*HMOX1*, *TBL1XR1*, *SCO2*, *CARM1*, *UBC*, *NCOA2*, *SIN3A*, *PSMB3*), mitochondria- and mitophagy-related pathways (*PMPCA*, *NDUFB7*, *NDUFS6*, *NDUFS3*, *NDUFV1*, *MCAT*, *COX17*, *TOMM5*, *TOMM40*, *HSPD1*, *TIMM50*, *UBC*), and many others. A full list of DEGs from DE-exposed control and AD OM cells that are part of AD-specific pathways in the Rotterdam Study is given in Supplementary Material S5, AD Significant Features.

In another analysis, we classified non-demented control individuals from the Rotterdam Study based on the pollution levels in their residential area (high pollution [HI] and low pollution [LO]). We aimed to detect clinical features and pathways specific to residents in highly polluted areas. The identification of the classes HI and LO was achieved by clustering samples by the first two principal components calculated on five pollution metrics, as described in Methods, under the Classification section. Using netDx we achieved a binary classification with an AUROC of 0.58.

We then explored pathways specific to HI residents, identifying 61 features, including 55 biological pathways, two clinical features (age and hypertension medication), and four metabolite groups (ketone bodies, aromatic amino acids, low-density and high-density lipoprotein ratios) (all listed in Supplementary Material S5, HI Significant Features). Notably, most of the pathways that were found as signature pathways for the HI group in the Rotterdam Study were also found to include DEGs detected in DE-exposed control and AD OM cells (p value < 0.05; median fold change control = 1.106, AD = 1.979). A full list of the genes and pathways detected in the HI group can be found in Supplementary Material S5, HI Significant Features. Strikingly, when we compared the biological pathways detected in HI residents from the Rotterdam Study with DE-exposed AD and control OM cells, we found, among other things, that the NRF2 pathway was involved in response to air pollution in all groups analyzed (Figure 7). Importantly, the NRF2 pathway was not only found to be a significant feature describing the HI group in the Rotterdam Study, but additionally many genes involved in the pathway were found to be deregulated upon exposure in both control and AD OM cells (Supplementary Material S5, HI Significant Features), confirming a key role of this pathway in air pollution response. Strikingly, we additionally found that pathways of influenza infection and viral RNA transcription were activated in AD and in control individuals exposed to high levels of pollution, and genes that are components of these pathways were also found to be altered in our study (Figure 7). As expected, we found a higher number of pathways having DEGs in AD-exposed OM cells compared to exposed controls (49 vs 33), with only one pathway being exclusive for controls (Figure 7). Among common pathways that were identified as significant in the HI group in the Rotterdam Study and that also had DEGs in both control and AD OM cells after DE exposure, we found pathways like a reactive oxygen species pathway, DNA repair pathway, and P53 pathway (Figure 7, Supplementary Material S5). These findings confirm our findings in vitro at a larger scale of population-based study data and consider the found pathways and gene targets significant features of response to air pollution.

In conclusion, when we assessed the overall analysis of the Rotterdam data, among the pathways identified in the AD compared to the control setting and in the comparison between pollution levels, the NRF2 pathway was the only overlapping identified feature. This finding highlights a key role of the NRF2 pathway in both AD disease pathogenesis and air pollution-induced responses.

4 | DISCUSSION

This study investigated the impact of DE exposure on OM cells from cognitively unimpaired individuals and individuals with AD using the ALI exposure system to mimic real-life conditions. Repeated low-level DE exposures induced significant transcriptomic responses, changes in miRNA and DNA methylation, and pathway activation. Cells with AD pathology showed heightened sensitivity, evidenced by a four-fold increase in the number of DEGs found. One of the key DEG families found altered in exposed AD cells was the NR4A family. This subfamily of nuclear receptors is critical for cellular homeostasis and DNA repair in health and disease.[68] mRNA levels of three members of this family, *NR4A1*, *NR4A2*, and *NR4A3*, were downregulated in DE-exposed AD cells, suggesting that TRAP exposure negatively impacts their protective functions. Interestingly, some of these DEGs were previously found to be downregulated in other models.[69–73] It is therefore plausible that these factors play a key role in pollution-mediated AD progression.

We additionally addressed the promising direction of research showing that miRNA profiling can be a great tool for studying both AD progression[57,58] and air pollution effects.[74,75] Integrating miRNA and mRNA expression data revealed that certain miRNAs, namely, miR-663a, miR-4792, and miR-508-5p in DE-exposed AD cells and miR-6828-5p and miR-1197 in the control exposed group, were inversely correlated with their target genes related to oxidative stress response. Additionally, we identified genes involved in the UPR with inverse correlations to their regulating miRNAs in both exposed groups: miR-601 in control cells and miR-1246 and miR-663a in AD cells. These findings highlight that certain targets are regulated at both mRNA and miRNA levels in toxicological responses to TRAP and suggest new miRNA targets for further research.

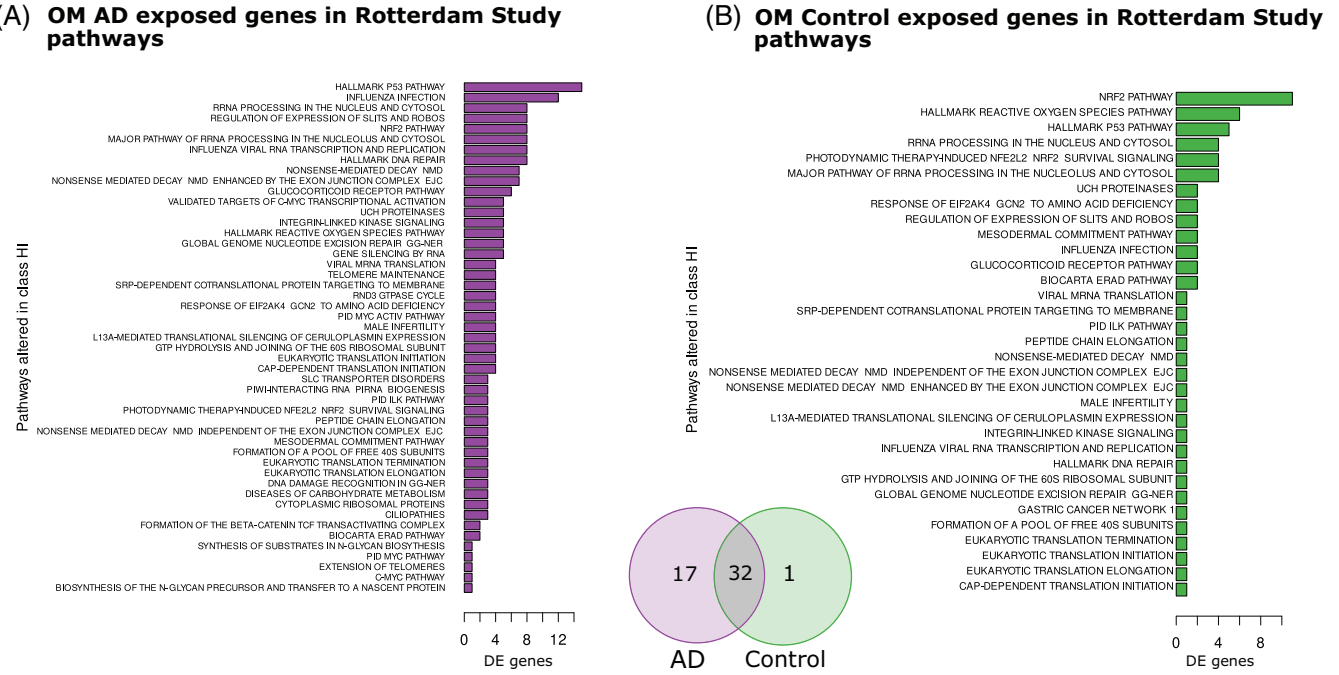

FIGURE 7 Number of DEGs in DE-exposed AD OM cells (A) and DE-exposed control OM cells (B) found in representative pathways of highly polluted areas whose residents participated in Rotterdam Study. Venn diagram represents overlap of the two pathway lists. AD, Alzheimer's disease; DE, diesel emissions; DEG, differentially expressed gene; OM, olfactory mucosa.

4.1 | Canonical pathways

Our findings align with previous studies proposing NRF2 transcription factor as a regulator of PM responses in both brain[76] and periphery. In DE-exposed control cells, we observed high activation of several components of the NRF2 pathway, as well as activation of the NRF2 transcription factor itself. We also found that a xenobiotic pathway was highly activated in DE-exposed control cells. This finding is in line with previous research highlighting the key role of this pathway in cell detoxification response to air pollutants, which was previously reported in various cell models exposed to PM.[77–79] For the first time, we report this pathway activation in exposure scenarios that are closer to real-life conditions and report this cell defense response in human OM cells. In contrast, DE-exposed AD cells showed dampened activation of both NRF2 and xenobiotic metabolism pathways. Deficient activation of these protective cell pathways in AD cells resulted in overall higher pathological responses, including the deregulation of a wide variety of genes and pathways such as UPR and ER stress response, eNOS, and apoptosis signaling.

Our results demonstrate that ER stress is highly activated by DE exposure in AD cells. Notably, activation of the ER stress pathway was previously reported after exposure to low levels of 1-nitropyrene, a PAH abundant in DE, in human epithelial cells.[80] Our findings are aligned with this study since our chemical analysis confirmed the presence of 1-nitropyrene in our samples.

HSPs are key players in protein folding and degradation, protecting cells from ER stress-induced apoptosis[81] and toxic stress induced by chemicals and metals.[82] Animal studies have indicated a major role of HSP activation in response to environmental contamination, as reviewed by Moreira-de-Sousa et al.,[83] highlighting HSP70 as an environmental contamination biomarker.[81] In this study, we found not only upregulation of several HSP70 family members' proteins in DE-exposed AD cells but also high activation of UPR and ER stress pathways and a significant increase in released HSP70 protein. We hypothesize that HSP70 induction may be protective against pathological processes induced by exposure, like unfolded protein aggregation and ER stress. The increment in HSP70 release in exposed AD cells found in our study indicates that HSP70 is not only upregulated inside cells but also actively released into the extracellular space.

4.2 | DNA methylation and DMRs-DEGs correlation

Overall, we found a slightly higher number of gene body methylation sites in DE-exposed AD cells than in control cells, with a higher number of hypomethylated genes in AD cells. In contrast, control cells had a significantly higher proportion of hypermethylated genes, including the Forkhead Box F1 (*FOXF1*) gene, which encodes a transcription factor important for extracellular matrix integrity. Previously, *FOXF1* hypermethylation was reported in toxicology,[84,85] highlighting the importance of this gene in response to environmental contaminants. Our data support the importance of FOXF1 in cell defense against metals and different xenobiotic components that are present in DE.

4.3 | Validation of results obtained in Rotterdam Study

Assessing the data from the Rotterdam Study, we analyzed AD- and air pollution-specific responses in a population-based cohort and integrated this analysis with our in vitro data. Classifying individuals in the Rotterdam Study based on disease incidence, we identified 115 significant features predictive of AD, including three clinical features and 112 biological pathways, such as amino acid transport, autophagy, inflammatory response, NRF2 pathway, respiratory electron transport, and many others. Then we performed a comparison of AD-specific pathways in participants from the Rotterdam Study with DEGs found in non-exposed AD OM cells compared to control OM cells and revealed striking similarities. This convergence, especially in key pathways associated with AD, reinforces the significance of these pathways and confirms the translational potential of this cell model.

We additionally analyzed which DEGs found in the in vitro study in DE-exposed control and AD cells were also components of AD-specific pathways found in the Rotterdam Study. This analysis allowed us to identify genes that were components of AD-specific pathways that were deregulated in control and AD OM cells upon exposure. The alignment confirmed the relevance of our in vitro findings to the AD-specific pathways identified in the Rotterdam Study.

To assess exclusively air pollution-specific responses in the Rotterdam Study, we classified non-demented individuals by pollution levels in their residential areas. We found 61 significant features, including biological pathways, clinical features, and metabolite groups, specific to HI residents. These features identified as specific to HI residents can provide important insights for future studies. Remarkably, many pathways identified as signatures for the HI group in the Rotterdam Study significantly overlapped with pathways found in DE-exposed control and AD OM cells, highlighting the impact of pollution. Overall, our analysis revealed that the NRF2 pathway emerged as a consistent response to air pollution exposures. Notably, this pathway not only was a predictive feature for the HI group in the Rotterdam Study but also showed consistent deregulation in exposed control and AD OM cells, emphasizing its pivotal role.

4.4 | Summary

The higher number of pathways with DEGs in AD-exposed OM cells compared to controls further underscores the unique and intensified response of AD cells to environmental stressors. Common pathways identified across population-based and in vitro studies, such as NRF2 pathway, reactive oxygen species pathway, DNA repair pathway, and P53 pathway, strengthen the robustness of our findings.

Overall, our findings reveal significant differences in the responses of control and AD OM cells to DE exposure, indicating that AD cells are more susceptible. Our integrative analysis successfully linked AD-specific and air pollution-specific pathways from the Rotterdam Study to OM cells and underscored the relevance of our findings. The consistent alignment of pathways and genes across these two datasets provides strong evidence for the role of the NRF2 pathway, xenobiotic metabolism, and other identified pathways in both AD and air pollution responses. This work provides a great example of validation of in vitro data in population-based human cohort studies for increasing the translational potential of research and successful identification of relevant systemic biological targets.

It must be noted that this study has several limitations. First, the absence of high-throughput proteomics limits our understanding of the downstream effects of the observed transcriptomic deregulation, making it difficult to assess the functional impact of DE exposure. Second, the in vitro study included only female donors, which does not adequately represent the population response due to potential gender differences in gene expression. Third, the experimental design lacks temporal resolution or variation in fuel types, restricting insights to time- and fuel-dependent transcriptomic responses to TRAP exposure or air pollution exposure in general. Lastly, multiomics analysis of biopsies and clinical material from individuals exposed to varying levels of TRAP over their lifespan would expand our understanding and provide the most relevant exposure scenario for studying TRAP effects. Future research addressing these limitations could offer a more holistic and in-depth understanding of the biological processes triggered by TRAP exposure in both health and AD.

As global air pollution rises, it is imperative to uncover and address its impact on human health, especially in vulnerable populations like AD individuals. Further investigation is warranted to validate and advance biomarker discovery for air pollution effects.

AUTHOR CONTRIBUTIONS

Conceptualization: Liudmila Saveleva, Sweelin Chew, Michal Vojtisek-Lom, Jan Topinka, Rosalba Giugno, Pavel Rössner, and Katja M Kanninen. *Investigation*: Liudmila Saveleva, Tereza Cervena, Claudia Mengoni, Michal Sima, Zdenek Krejcik, Kristyna Vrbova, Jitka Sikorova, Laura Mussalo, Mariia Ivanova, Zuzana Šímová, Ali Shahbaz, and Michal Vojtisek-Lom. *Validation*: Liudmila Saveleva, Mariia Ivanova, and Ali Shahbaz. *Writing—original draft*: Liudmila Saveleva and Claudia Mengoni. *Visualization*: Liudmila Saveleva and Claudia Mengoni. *Project administration*: Liudmila Saveleva, Tereza Cervena, Sweelin Chew, Michal Vojtisek-Lom, Jan Topinka, Rosalba Giugno, Pavel Rössner, and Katja M. Kanninen. *Supervision*: Tereza Cervena. *Writing—review and editing*: Tereza Cervena, Claudia Mengoni, Michal Sima, Zdenek Krejcik, Kristyna Vrbova, Tosca de Crom, Tarja Malm, Michal Vojtisek-Lom, Pavel Rössner, and Katja M. Kanninen. *Formal analysis*: Claudia Mengoni, Kristyna Vrbova, and Jitka Sikorova. *Data curation*: Claudia Mengoni, Zdenek Krejcik, and Tosca de Crom. *Resources*: Elina Penttilä, Heikki Löppönen, Anne M. Koivisto, Arfan Ikram, Michal Vojtisek-Lom, Jan Topinka, Rosalba Giugno, Pavel Rössner, and Katja M. Kanninen. *Methodology*: Pasi I Jalava, Michal Vojtisek-Lom, Jan Topinka, Pavel Rössner, and Katja M. Kanninen. *Funding acquisition*: Tarja Malm, Jan Topinka, Rosalba Giugno, Pavel Rössner, and Katja M. Kanninen. *Supervision*: Jan Topinka, Rosalba Giugno, Pavel Rössner, and Katja M. Kanninen.

ACKNOWLEDGMENTS

The authors would like to thank Dr. Luca Giudice for his help in addressing reviewer comments, Dr. Riikka Lampinen for her help in preparing cell cultures, MSc Ravi Teja Kondaveeti and Houssein Nasser for their help with the literature search, and MSc Emma Gribchenko for her help with addressing reviewer comments. This is an EU Joint Programme—Neurodegenerative Disease Research (JPND) project. This research was supported by the ADAIR project (Grant JPND2019-466-037). This publication is connected to work from COST Action CA20121, BenBedPhar, supported by COST (European Cooperation in Science and Technology). The authors acknowledge the assistance provided by the Research Infrastructure NanoEnviCz, supported by the Ministry of Education, Youth, and Sports of the Czech Republic under Project LM2023066 and the Research Infrastructure EATRIS-CZ, supported by the Ministry of Education, Youth, and Sports of the Czech Republic under Project LM2023053. The development of an improved air–liquid interface exposure system was supported by Czech Science Foundation Grant 22-10279S. This work was further supported by the Ministry of Education, Youth, and Sports of the Czech Republic and The European Union—European Structural and Investments Funds in the frame of Operational Programme Research Development and Education—project Pro-NanoEnviCz (Project CZ.02.1.01/0.0/0.0/16_013/0001821), the Doctoral Program in Molecular Medicine at the University of Eastern Finland, the Kuopio University Foundation, and the North Savo Regional Fund of the Finnish Cultural Foundation Grant 65231471. Further funding was obtained from the Stichting Erasmus Trustfonds, Grant 97030.2021.101.430/057/RB. This study was also partly funded through the Netherlands Organisation for Health Research and Development (ZonMW) Grant 733051107.

CONFLICT OF INTEREST STATEMENT

The authors have no conflicts of interest to declare. Author disclosures are available in the Supporting Information.

CONSENT STATEMENT

Informed consent was obtained from all subjects involved in the study.

REFERENCES

1. Yu W, Ye T, Zhang Y, et al. Global estimates of daily ambient fine particulate matter concentrations and unequal spatiotemporal distribution of population exposure: a machine learning modelling study. *Lancet Planet Health*. 2023;7(3):e209-e218. doi:10.1016/S2542-5196(23)00008-6
2. Cory-Slechta DA, Sobolewski M. Neurotoxic effects of air pollution: an urgent public health concern. *Nat Rev Neurosci*. 2023;24:129-130. doi:10.1038/s41583-022-00672-8
3. Ferreira APS, Ramos JMO, Gamaro GD, Gioda A, Gioda CR, Souza ICC. Experimental rodent models exposed to fine particulate matter (PM2.5) highlighting the injuries in the central nervous system: a systematic review. *Atmos Pollut Res*. 2022;13(5):101407. doi:10.1016/J.APR.2022.101407
4. Kilian J, Kitazawa M. The emerging risk of exposure to air pollution on cognitive decline and Alzheimer's disease—evidence from epidemiological and animal studies. *Biomed J*. 2018;41(3):141-162. doi:10.1016/j.bj.2018.06.001
5. Duchesne J, Gutierrez LA, Carrière I, et al. Exposure to ambient air pollution and cognitive decline: results of the prospective three-city cohort study. *Environ Int*. 2022;161:107118. doi:10.1016/J.ENVINT.2022.107118
6. O'Piela DR, Durisek GR, Escobar YNH, Mackos AR, Wold LE. Particulate matter and Alzheimer's disease: an intimate connection. *Trends Mol Med*. 2022;28:770-780. doi:10.1016/J.MOLMED.2022.06.004
7. Livingston G, Huntley J, Sommerlad A, et al. Dementia prevention, intervention, and care: 2020 report of the Lancet Commission. *Lancet*. 2020;396(10248):413-446. doi:10.1016/S0140-6736(20)30367-6
8. Ajmani GS, Suh HH, Pinto JM. Effects of ambient air pollution exposure on olfaction: a review. *Environ Health Perspect*. 2016;124(11):1683-1693. doi:10.1289/EHP136
9. Liang C, Jiang Y, Zhang T, et al. Atmospheric particulate matter impairs cognition by modulating synaptic function via the nose-to-brain route. *Sci Total Environ*. 2022;857:159600. doi:10.1016/J.SCITOTENV.2022.159600
10. Kim SJ, Kim N, Park SH, et al. Genomic approach to explore altered signaling networks of olfaction in response to diesel exhaust particles in mice. *Sci Rep*. 2020;10(1):16972. doi:10.1038/S41598-020-74109-6
11. Vondráček J, Pěnčíková K, Neča J, et al. Assessment of the aryl hydrocarbon receptor-mediated activities of polycyclic aromatic hydrocarbons in a human cell-based reporter gene assay. *Environ Pollut*. 2017;220(Pt A):307-316. doi:10.1016/J.ENVPOL.2016.09.064
12. Kanninen KM, Lampinen R, Rantanen LM, et al. Olfactory cell cultures to investigate health effects of air pollution exposure: implications for neurodegeneration. *Neurochem Int*. 2020;136:104729. doi:10.1016/j.neuint.2020.104729
13. Lampinen R, Fazaludeen MF, Avesani S, et al. Single-Cell RNA-seq analysis of olfactory mucosal cells of Alzheimer's disease patients. *Cells*. 2022;11(4):676. doi:10.3390/CELLS11040676
14. Lampinen R, Górová V, Avesani S, et al. Biometal Dyshomeostasis in olfactory mucosa of Alzheimer's disease patients. *Int J Mol Sci*. 2022;23(8):4123. doi:10.3390/IJMS23084123
15. Mussalo L, Avesani S, Shahbaz MA, et al. Emissions from modern engines induce distinct effects in human olfactory mucosa cells, depending on fuel and aftertreatment. *Sci Total Environ*. 2023;905:167038. doi:10.1016/j.scitotenv.2023.167038
16. Rossner P, Cervena T, Vojtisek-Lom M. In vitro exposure to complete engine emissions—a mini-review. *Toxicology*. 2021;462:152953. doi:10.1016/J.TOX.2021.152953
17. Rossner P, Cervena T, Vojtisek-Lom M, et al. The biological effects of complete gasoline engine emissions exposure in a 3d human airway model (MucilAir^{TM}) and in human bronchial epithelial cells (BEAS-2B). *Int J Mol Sci*. 2019;20(22):5710. doi:10.3390/IJMS20225710
18. Vojtisek-Lom M, Pechout M, MacOun D, et al. Assessing exhaust toxicity with biological detector: configuration of portable air-liquid interface human lung cell model exposure system, sampling train and test conditions. *SAE Int J Adv Curr Pract Mobil*. 2019;2(2):520-534. doi:10.4271/2019-24-0050
19. Cervena T, Vojtisek-Lom M, Vrbova K, et al. Ordinary gasoline emissions induce a toxic response in bronchial cells grown at air-liquid interface. *Int J Mol Sci*. 2020;22(1):79. doi:10.3390/IJMS22010079
20. Libalova H, Rossner P, Vrbova K, et al. Comparative analysis of toxic responses of organic extracts from diesel and selected alternative fuels engine emissions in human lung BEAS-2B cells. *Int J Mol Sci*. 2016;17(11):1833. doi:10.3390/IJMS17111833
21. Dobin A, Davis CA, Schlesinger F, et al. STAR: ultrafast universal RNA-seq aligner. *Bioinformatics*. 2013;29(1):15-21. doi:10.1093/BIOINFORMATICS/BTS635
22. Robinson MD, McCarthy DJ, Smyth GK. edgeR: a Bioconductor package for differential expression analysis of digital gene expression data. *Bioinformatics*. 2010;26(1):139-140. doi:10.1093/BIOINFORMATICS/BTP616

23. Ritchie ME, Phipson B, Wu D, et al. limma powers differential expression analyses for RNA-sequencing and microarray studies. *Nucleic Acids Res*. 2015;43(7):e47. doi:10.1093/NAR/GKV007
24. Wu T, Hu E, Xu S, et al. clusterProfiler 4.0: a universal enrichment tool for interpreting omics data. *Innovation*. 2021;2(3):100141. doi:10.1016/J.XINN.2021.100141
25. Krämer A, Green J, Pollard J, Tugendreich S. Causal analysis approaches in Ingenuity Pathway Analysis. *Bioinformatics*. 2014;30(4):523-530. doi:10.1093/BIOINFORMATICS/BTT703
26. Bioconductor. miRNAtap. 2024. Accessed September 25, 2023. https://bioconductor.org/packages/release/bioc/html/miRNAtap.html
27. Wong N, Wang X. miRDB: an online resource for microRNA target prediction and functional annotations. *Nucleic Acids Res*. 2015;43:D146-D152. doi:10.1093/NAR/GKU1104
28. Maragkakis M, Vergoulis T, Alexiou P, et al. DIANA-microT Web server upgrade supports fly and worm miRNA target prediction and bibliographic miRNA to disease association. *Nucleic Acids Res*. 2011;39:W145-W148. doi:10.1093/NAR/GKR294
29. Reczko M, Maragkakis M, Alexiou P, Grosse I, Hatzigeorgiou AG. Functional microRNA targets in protein coding sequences. *Bioinformatics*. 2012;28(6):771-776. doi:10.1093/BIOINFORMATICS/BTS043
30. Friedman RC, Farh KK, Burge CB, Bartel DP. Most mammalian mRNAs are conserved targets of microRNAs. *Genome Res*. 2009;19(1):92-105. doi:10.1101/GR.082701.108
31. Lall S, Grün D, Krek A, et al. A genome-wide map of conserved MicroRNA targets in C. elegans. *Curr Biol*. 2006;16(5):460-471. doi:10.1016/j.cub.2006.01.050
32. Betel D, Koppal A, Agius P, Sander C, Leslie C. Comprehensive modeling of microRNA targets predicts functional non-conserved and non-canonical sites. *Genome Biol*. 2010;11(8):R90. doi:10.1186/GB-2010-11-8-R90/FIGURES/6
33. John B, Enright AJ, Aravin A, Tuschl T, Sander C, Marks DS. Human MicroRNA targets. *PLoS Biol*. 2004;2(11):e363. doi:10.1371/JOURNAL.PBIO.0020363
34. Enright AJ, John B, Gaul U, Tuschl T, Sander C, Marks DS. MicroRNA targets in drosophila. *Genome Biol*. 2003;5(1):R1. doi:10.1186/GB-2003-5-1-R1
35. Ikram MA, Brusselle G, Ghanbari M, et al. Objectives, design and main findings until 2020 from the Rotterdam Study. *Eur J Epidemiol*. 2020;35(5):483-517. doi:10.1007/S10654-020-00640-5
36. de Crom TOE, Ginos BNR, Oudin A, Ikram MK, Voortman T, Ikram MA. Air pollution and the risk of dementia: the Rotterdam Study. *J Alzheimers Dis*. 2023;91(2):603-613. doi:10.3233/JAD-220804
37. Vojinovic D, van der Lee SJ, van Duijn CM, et al. Metabolic profiling of intra- and extracranial carotid artery atherosclerosis. *Atherosclerosis*. 2018;272:60-65. doi:10.1016/j.atherosclerosis.2018.03.015
38. Richards J, Rivadeneira F, Inouye M, et al. Bone mineral density, osteoporosis, and osteoporotic fractures: a genome-wide association study. *Lancet*. 2008;371(9623):1505-1512. doi:10.1016/S0140-6736(08)60599-1
39. van den Berg RA, Hoefsloot HCJ, Westerhuis JA, Smilde AK, van der Werf MJ. Centering, scaling, and transformations: improving the biological information content of metabolomics data. *BMC Genomics*. 2006;7:142. doi:10.1186/1471-2164-7-142
40. Purcell S, Neale B, Todd-Brown K, et al. PLINK: a tool set for whole-genome association and population-based linkage analyses. *Am J Hum Genet*. 2007;81(3):559-579. doi:10.1086/519795
41. Naj AC, Jun G, Beecham GW, et al. Common variants at MS4A4/MS4A6E, CD2AP, CD33 and EPHA1 are associated with late-onset Alzheimer's disease. *Nat Genet*. 2011;43(5):436-441. doi:10.1038/ng.801
42. Merico D, Isserlin R, Stueker O, Emili A, Bader GD. Enrichment map: a network-based method for gene-set enrichment visualization and interpretation. *PLoS One*. 2010;5(11):e13984. doi:10.1371/JOURNAL.PONE.0013984
43. Kunkle BW, Grenier-Boley B, Sims R, et al. Genetic meta-analysis of diagnosed Alzheimer's disease identifies new risk loci and implicates Aβ, tau, immunity and lipid processing. *Nat Genet*. 2019;51(3):414-430. doi:10.1038/s41588-019-0358-2
44. Lambert JC, Ibrahim-Verbaas CA, Harold D, et al. Meta-analysis of 74,046 individuals identifies 11 new susceptibility loci for Alzheimer's disease. *Nat Genet*. 2013;45(12):1452-1458. doi:10.1038/ng.2802
45. Hollingworth P, Harold D, Sims R, et al. Common variants in ABCA7, MS4A6A/MS4A4E, EPHA1, CD33 and CD2AP are associated with Alzheimer's disease. *Nat Genet*. 2011;43(5):429-435. doi:10.1038/NG.803
46. Pai S, Weber P, Isserlin R, et al. netDx: software for building interpretable patient classifiers by multi-'omic data integration using patient similarity networks. *F1000Research*. 2020;9:1239. doi:10.12688/f1000research.26429.2
47. Pai S, Hui S, Isserlin R, et al. netDx: interpretable patient classification using integrated patient similarity networks. *Mol Syst Biol*. 2019;15(3):e8497. doi:10.15252/MSB.20188497
48. Finckh U, van Hadeln K, Müller-Thomsen T, et al. Association of late-onset Alzheimer disease with a genotype of PLAU, the gene encoding urokinase-type plasminogen activator on chromosome 10q22.2. *Neurogenetics*. 2003;4(4):213-217. doi:10.1007/S10048-003-0157-9/FIGURES/1
49. Cuyvers E, van der Zee J, Bettens K, et al. Genetic variability in SQSTM1 and risk of early-onset Alzheimer dementia: a European early-onset dementia consortium study. *Neurobiol Aging*. 2015;36(5):2005.e15-2005.e22. doi:10.1016/J.NEUROBIOLAGING.2015.02.014
50. Tramutola A, Di Domenico F, Barone E, Perluigi M, Butterfield DA. It is all about (U)biquitin: role of altered ubiquitin-proteasome system and UCHL1 in alzheimer disease. *Oxid Med Cell Longev*. 2016;2016:2756068. doi:10.1155/2016/2756068
51. Liu D, Wang Y, Jing H, Meng Q, Yang J. Mendelian randomization integrating GWAS and DNA methylation quantitative trait loci data identified novel pleiotropic DNA methylation loci for neuropathology of Alzheimer's disease. *Neurobiol Aging*. 2021;97:18-27. doi:10.1016/J.NEUROBIOLAGING.2020.09.019
52. Chen Y, Zhou H, binYin W, Ren H. Construction of a new protein–protein interaction and molecular biomarkers networks in Alzheimer's disease patients by bioinformatics screening. *J Biomed Nanotechnol*. 2023;19(1):154-171. doi:10.1166/JBN.2023.3507
53. He F, Ru X, Wen T. NRF2, a transcription factor for stress response and beyond. *Int J Mol Sci*. 2020;21(13):4777. doi:10.3390/IJMS21134777
54. Buendia I, Michalska P, Navarro E, Gameiro I, Egea J, León R. Nrf2-ARE pathway: an emerging target against oxidative stress and neuroinflammation in neurodegenerative diseases. *Pharmacol Ther*. 2016;157:84-104. doi:10.1016/J.PHARMTHERA.2015.11.003
55. Ngo V, Duennwald ML. Nrf2 and oxidative stress: a general overview of mechanisms and implications in human disease. *Antioxidants*. 2022;11(12):2345. doi:10.3390/ANTIOX11122345
56. Morales-Bárcenas R, Sánchez-Pérez Y, Santibáñez-Andrade M, Chirino YI, Soto-Reyes E, García-Cuellar CM. Airborne particulate matter (PM10) induces cell invasion through aryl hydrocarbon receptor and activator protein 1 (AP-1) pathway deregulation in A549 lung epithelial cells. *Mol Biol Rep*. 2023;50(1):107-119. doi:10.1007/S11033-022-07986-X/FIGURES/5
57. Pichler S, Gu W, Hartl D, et al. The miRNome of Alzheimer's disease: consistent downregulation of the miR-132/212 cluster. *Neurobiol Aging*. 2017;50:167.e1-167.e10. doi:10.1016/J.NEUROBIOLAGING.2016.09.019
58. Lau P, Bossers K, Janky R, et al. Alteration of the microRNA network during the progression of Alzheimer's disease. *EMBO Mol Med*. 2013;5(10):1613-1634. doi:10.1002/EMMM.201201974

59. Song Y, He S, Zhuang J, et al. MicroRNA-601 serves as a potential tumor suppressor in hepatocellular carcinoma by directly targeting PIK3R3. *Mol Med Rep*. 2023;27:36. doi:10.3892/MMR.2019.9857/HTML
60. Sun B, Hua J, Cui H, Liu H, Zhang K, Zhou H. MicroRNA-1197 down-regulation inhibits proliferation and migration in human non- small cell lung cancer cells by upregulating HOXC11. *Biomed Pharmacother*. 2019;117:109041. doi:10.1016/J.BIOPHA.2019.109041
61. Huang X, Tang F, Weng Z, Zhou M, Zhang Q. MiR-591 functions as tumor suppressor in breast cancer by targeting TCF4 and inhibits Hippo-YAP/TAZ signaling pathway. *Cancer Cell Int*. 2019;19(1):108. doi:10.1186/S12935-019-0818-X/FIGURES/6
62. Song MK, Lee HS, Ryu JC. Integrated analysis of microRNA and mRNA expression profiles highlights aldehyde-induced inflammatory responses in cells relevant for lung toxicity. *Toxicology*. 2015;334:111-121. doi:10.1016/J.TOX.2015.06.007
63. Moore LD, Le T, Fan G. DNA methylation and its basic function. *Neuropsychopharmacology*. 2012;38(1):23-38. doi:10.1038/npp.2012.112
64. De Prins S, Koppen G, Jacobs G, et al. Influence of ambient air pollution on global DNA methylation in healthy adults: a seasonal follow-up. *Environ Int*. 2013;59:418-424. doi:10.1016/J.ENVINT.2013.07.007
65. Huo X, Sun H, Cao D, et al. Identification of prognosis markers for endometrial cancer by integrated analysis of DNA methylation and RNA-Seq data. *Sci Rep*. 2019;9(1):9924. doi:10.1038/s41598-019-46195-8
66. Huang SK, Tripathi P, Koneva LA, et al. Effect of concentration and duration of particulate matter exposure on the transcriptome and DNA methylome of bronchial epithelial cells. *Environ Epigenet*. 2021;7(1):dvaa022. doi:10.1093/EEP/DVAA022
67. Zhu W, Gu Y, Li M, et al. Integrated single-cell RNA-seq and DNA methylation reveal the effects of air pollution in patients with recurrent spontaneous abortion. *Clin Epigenetics*. 2022;14(1):105. doi:10.1186/S13148-022-01327-2/TABLES/3
68. Safe S, Jin UH, Morpurgo B, Abudayyeh A, Singh M, Tjalkens RB. Nuclear receptor 4A (NR4A) family—orphans no more. *J Steroid Biochem Mol Biol*. 2016;157:48-60. doi:10.1016/J.JSBMB.2015.04.016
69. Navarro JF, Croteau DL, Jurek A, et al. Spatial transcriptomics reveals genes associated with dysregulated mitochondrial functions and stress signaling in Alzheimer disease. *iScience*. 2020;23(10):101556. doi:10.1016/J.ISCI.2020.101556
70. Zhao LG, Tang Y, Tan JZ, Wang JW, Chen GJ, Zhu BL. The effect of NR4A1 on APP metabolism and tau phosphorylation. *Genes Dis*. 2018;5(4):342-348. doi:10.1016/J.GENDIS.2018.04.008
71. Parra-Damas A, Valero J, Chen M, et al. Crtc1 activates a transcriptional program deregulated at early Alzheimer's disease-related stages. *J Neurosci*. 2014;34(17):5776-5787. doi:10.1523/JNEUROSCI.5288-13.2014
72. Montarolo F, Perga S, Martire S, et al. Altered NR4A subfamily gene expression level in peripheral blood of Parkinson's and Alzheimer's disease patients. *Neurotox Res*. 2016;30(3):338-344. doi:10.1007/S12640-016-9626-4/TABLES/2
73. Jeon SG, Yoo A, Chun DW, et al. The critical role of nurr1 as a mediator and therapeutic target in Alzheimer's disease-related pathogenesis. *Aging Dis*. 2020;11(3):705-724. doi:10.14336/AD.2019.0718
74. Jardim MJ. microRNAs: implications for air pollution research. *Mutat Res*. 2011;717(1-2):38-45. doi:10.1016/J.MRFMMM.2011.03.014
75. Krauskopf J, van Veldhoven K, Chadeau-Hyam M, et al. Short-term exposure to traffic-related air pollution reveals a compound-specific circulating miRNA profile indicating multiple disease risks. *Environ Int*. 2019;128:193-200. doi:10.1016/J.ENVINT.2019.04.063
76. Haghani A, Cacciottolo M, Doty KR, et al. Mouse brain transcriptome responses to inhaled nanoparticulate matter differed by sex and APOE in Nrf2-Nfkb interactions. *Elife*. 2020;9:e54822. doi:10.7554/eLife.54822
77. Kampa M, Castanas E. Human health effects of air pollution. *Environ Pollut*. 2008;151(2):362-367. doi:10.1016/J.ENVPOL.2007.06.012
78. Lepers C, André V, Dergham M, et al. Xenobiotic metabolism induction and bulky DNA adducts generated by particulate matter pollution in BEAS-2B cell line: geographical and seasonal influence. *J Appl Toxicol*. 2014;34(6):703-713. doi:10.1002/JAT.2931
79. Líbalová H, Krčková S, Uhlířová K, et al. Analysis of gene expression changes in A549 cells induced by organic compounds from respirable air particles. *Mutat Res*. 2014;770:94-105. doi:10.1016/J.MRFMMM.2014.10.002
80. Andersson H, Piras E, Demma J, Hellman B, Brittebo E. Low levels of the air pollutant 1-nitropyrene induce DNA damage, increased levels of reactive oxygen species and endoplasmic reticulum stress in human endothelial cells. *Toxicology*. 2009;262(1):57-64. doi:10.1016/J.TOX.2009.05.008
81. Laing S, Wang G, Briazova T, et al. Airborne particulate matter selectively activates endoplasmic reticulum stress response in the lung and liver tissues. *Am J Physiol Cell Physiol*. 2010;299(4):C736-C749. doi:10.1152/AJPCELL.00529.2009
82. Hu C, Yang J, Qi Z, et al. Heat shock proteins: biological functions, pathological roles, and therapeutic opportunities. *MedComm*. 2022;3(3):e161. doi:10.1002/MCO2.161
83. Moreira-de-Sousa C, de Souza RB, Fontanetti CS. HSP70 as a biomarker: an excellent tool in environmental contamination analysis—a review. *Water Air Soil Pollut*. 2018;229(8):264. doi:10.1007/S11270-018-3920-0/TABLES/1
84. Smeester L, Rager JE, Bailey KA, et al. Epigenetic changes in individuals with arsenicosis. *Chem Res Toxicol*. 2011;24(2):165-167. doi:10.1021/TX1004419/SUPPL_FILE/TX1004419_SI_001.PDF
85. Lee JY, Tokumoto M, Fujiwara Y, et al. Accumulation of p53 via down-regulation of UBE2D family genes is a critical pathway for cadmium-induced renal toxicity. *Sci Rep*. 2016;6(1):21968. doi:10.1038/srep21968

SUPPORTING INFORMATION

Additional supporting information can be found online in the Supporting Information section at the end of this article.

How to cite this article: Saveleva L, Cervena T, Mengoni C, et al. Transcriptomic and epigenomic profiling reveals altered responses to diesel emissions in Alzheimer's disease both in vitro and in population-based data. *Alzheimer's Dement*. 2024;20:8825–8843. https://doi.org/10.1002/alz.14347